EXTENSIONS OF ASYMPTOTIC WEDGE DIFFRACTION THEORY

A Dissertation

Presented to

The Faculty of Graduate Studies

The University of Manitoba

In Partial Fulfillment

of the Requirements for the Degree

Doctor of Philosophy

by

ADEL A.K. MANSOUR MOHSEN

July 1971

ABSTRACT

The problem of asymptotic diffraction of waves by a perfectly conducting wedge, with and without dielectric loading, is treated in this thesis. The dielectric loading is in the form of a slab on the illuminated side of the wedge. The thickness of the slab is assumed small relative to the wavelength and its relative permittivity is assumed not much larger than unity. The solutions for the field are expressed in integral form and consist of geometrical optics terms and diffraction integrals. The saddle point method of integration is used to obtain asymptotic expressions for the diffraction integrals involved, in terms of Fresnel's integral. The accuracy of the asymptotic solution for the unloaded case is established by favorable comparison with previous results derived by Pauli, Oberhettinger and Hutchins, as well as with available exact solutions. The validity of the results for the loaded wedge is verified by good agreement with experiment for the case of a dipole-fed strip loaded with a dielectric slab. Apart from the significant effect of the dielectric slab on the radiation characteristics of the strip, the analysis shows how the edge rays influence the optimum thickness of the slab for given strip width, location of the source and relative permittivity.

ACKNOWLEDGEMENTS

The author wishes to thank Professor M.A.K. Hamid of the Electrical Engineering Department who proposed the topic and supervised the research throughout.

Thanks are also due to Dr. W.M. Boerner, Mr. R. Strelesky and other staff members of the Antenna Laboratory, for their assistance and to Mrs. P. Magel for excellent typing of the manuscript.

The use of the computing facilities at the University of Manitoba is also acknowledged.

The financial support of the National Research Council of Canada in the form of Research Grant (A3326) and of the Defence Research Board (Grant 3801-42) is deeply appreciated.

TABLE OF CONTENTS

LIST OF FIGURES

CHAPTER 1

INTRODUCTION

The exact solutions for a large number of diffraction problems have not been derived due to the lack of appropriate mathematical tools. In such cases, experimental, numerical or approximate analytical techniques have been commonly used with varying degrees of success.

A promising method at high frequencies is the ray optical technique or the geometrical theory of diffraction proposed by J. B. Keller [1-3]. The ordinary geometrical optics method is the oldest theory of light propagation. It assumes that light propagates along rays according to Fermat's principle,which postulates that the rays between two points are those curves along which the optical path length is stationary with respect to infinitesimal variations in path [4, p. 340]. However, geometrical optics fails to account for the existence of the field in the shadow regions, e.g. in the dark regions of illuminated opaque bodies. The geometrical theory of diffraction takes into account these fields by postulating that, in addition to the more classical incident, reflected and refracted rays of geometrical optics, there is a new class of rays called the diffracted rays. These rays are excited when an incident

ray strikes an edge, vertex or corner on the scatterer, or when it impinges tangentially on a smoothly curved boundary. Diffracted rays may also arise when total reflection is possible (lateral rays) or when a region of space is penetrated only by evanescent fields (evanescent rays) [5]. The computation of the total field at any observation point is conveniently performed by the use of the ray optical method once the ray diagram is traced,and only the sum contribution of the rays passing through the observation point needs to be taken into account.

The direction of propagation of the diffracted rays is determined by the generalized Fermat's principle [3]. Keller's modification of Fermat's principle for edge diffraction states that an edge diffracted ray from a point P to a point Q is a curve which has stationary optical length among all curves from P to Q with one point on the edge. The phase of the field on a diffracted ray is assumed to be proportional to the path length of the ray relative to a reference point where the phase is known. The amplitude of the field is assumed to change according to the principle of conservation of energy. The strength of the field depends on the incident field as well as the surface properties, such as curvature and type of material, in the neighborhood of the point of diffraction. The initial value of the field on a diffracted ray is obtained by multiplying the field on the incident ray by a diffraction coefficient. In the case of vector

fields the diffraction coefficient is a matrix which takes into account the direction and polarization of the field. Since only the local surface properties near the diffracting point are important, the diffraction coefficients may be determined from the asymptotic solution of the simplest boundary value problem having the same local properties, such as the wedge for edge diffraction [3] and the circular cylinder and sphere for diffraction by a convex surface [6]. Such boundary value problems are called characteristic or canonical problems.

The diffraction of waves by a wedge is fundamental to the application of the ray optical method to antennas or scattering bodies which have multiple edges. Thus, the wedge geometry has been encountered in problems involving apertures [7-10], antennas [11-19], waveguide structures [20-31] as well as many diffracting bodies [32-42]. In particular, the leading term of the asymptotic expansion of the exact solution for the diffracted field due to plane wave incidence on a perfectly conducting wedge [43] adequately describes the diffracted field at points well removed from the edge and transition boundaries (i.e. shadow and reflection boundaries). Since this term may be interpreted as a ray field, the approximate solution for bodies with multiple edges may be conveniently obtained, once the ray diagram is constructed, by taking into account the rays passing through the observation point.

In general, the basic advantages of the geometrical theory of diffraction are its conceptual simplicity and its ability to provide physical insight into the mechanisms of diffraction. Although the ray approach, based on this theory, is an asymptotic high frequency technique, it often gives accurate results when the characteristic dimension of the scatterer is of the order of the wavelength [3, 8, 26].

It should be noted, however, that certain computational difficulties arise in applying the ray method as originally proposed by Keller. One such difficulty is the accuracy of the field in the vicinity of transition boundaries where the usual ray edge diffraction coefficient [3] fails to provide satisfactory results. The reason for this is that the asymptotic evaluation used to obtain the diffraction coefficient fails in these transition regions [13]. Thus, the use of the usual plane wave edge diffraction coefficient led to strong disagreement with experiment in some applications [15]. Several investigations have been carried out in recent years to overcome this difficulty. Buchal and Keller [44] used a boundary layer method to deal with transition regions. However, this method divides space into various regions and yields separate expansions in each, which requires somewhat elaborate computations. Ahluwalia *et al.* [45] proposed a single uniform asymptotic expansion for the half-plane case, which uses a special function closely related to the Fresnel integrals. Yu and Rudduck

[34] applied Pauli's asymptotic solution [43] to the plane wave diffraction by a conducting strip. Yee *et al.* [26] used a Fresnel integral formula for the diffraction coefficient to provide a continuous transition of the diffracted field through the reflection boundary of an open-ended waveguide. Lewin [46] treated the problem of diffraction of H-polarized cylindrical waves by a wedge, with emphasis on the asymptotic expressions in transition regions, and successfully applied the solution to study the propagation in an overmoded right-angle corner [29].

A second difficulty arises in certain bodies where interacting edges are separated by relatively short distances in comparison to the wavelength. Such problems require modification of the diffraction coefficients to make them appropriate for the wave-fronts at each point in the multiple diffraction process. Previous attempts to overcome this difficulty were reported by many authors [16, 26, 29, 34, 39, 46]. Hamid [16] presented amplitude and phase correction factors in the diffraction coefficient by comparison with the exact solution. Morse [39] expressed the nonplanar edge wave in terms of linear combinations of plane waves and their derivatives. Mohsen and Hamid [9, 35] showed the significance of including higher order terms in the diffraction coefficients for plane wave incidence on a slit, circular aperture and a strip. The cylindrical, rather than plane wave, nature of edge diffracted fields was emphasized

by Kinber [13] and Rudduck [21]. Ufimtsev [33] used an asymptotic integral solution, in terms of Fresnel integrals, to evaluate the edge-edge interactions for a plane wave incident on a strip. Pauli's asymptotic solution for plane wave diffraction by a wedge [43] was successfully applied to horns [15] and strips [34].

One of the main purposes of this thesis is to derive accurate and easily computable asymptotic expressions for the diffracted field by a perfectly conducting wedge due to plane, cylindrical, and spherical wave excitations which are valid in transition regions as well as in the near field.

A third type of difficulty arises from the lack of solutions of canonical problems for other wedge configurations, particularly, the problem of the dielectric-loaded wedge. This problem is investigated in the present work for the case of a thin uniform dielectric slab which covers the illuminated side of the wedge and has a low relative dielectric constant, (i.e. not much larger than unity).

Summary

Since asymptotic wedge diffraction is necessary for the ray optical analysis of problems where edges are encountered, two contributions are presented in this thesis in order to improve the accuracy of the technique and to extend its applicability.

In Chapter 2, the problem of diffraction of plane, cylindrical and spherical waves by a perfectly conducting wedge is treated by a unified approach. Thus, starting from the series solution for cylindrical wave incidence and using an integral expression for products of the modified Bessel functions involved, the total field is represented as a geometrical optics term plus a diffraction integral. Using an integral form for the field of a spherical wave, the solution for the cylindrical wave excitation is extended to the spherical wave case. The result for plane wave excitation is deduced from the cylindrical wave result by letting the observation point tend to infinity. The saddle point method of integration is used to evaluate the diffraction integrals asymptotically in terms of Fresnel's integral. The accuracy of the results is tested by comparison with available exact and approximate solutions.

In order to extend the applicability of the ray optical technique to a dielectric-loaded wedge, the problem of diffraction of plane waves by a perfectly conducting wedge, having one side loaded with a thin dielectric slab

whose relative permittivity is not much larger than unity, is treated in Chapter 3. An approximate boundary condition at the dielectric surface is introduced and an integral representation of the field is used to obtain an approximate solution. Diffraction integrals of the type found in Chapter 2 are obtained and evaluated using the saddle point technique. Using the reciprocity principle, the results are extended to cylindrical wave excitation in order to obtain the far field.

In Chapter 4, the results of Chapter 3 are used to calculate the radiation pattern of a dielectric-loaded strip symmetrically-fed by a dipole. The validity of the technique is tested by comparison with experiments for different loading parameters.

Finally, the results are discussed in Chapter 5 while the conclusions and suggestions for future research are presented in Chapter 6.

CHAPTER 2

DIFFRACTION OF WAVES BY A CONDUCTING WEDGE

2.1 Introduction

The problem of diffraction of time harmonic waves by a perfectly conducting wedge has been the subject of numerous theoretical studies. The usual types of incident waves considered in these studies are plane, cylindrical or spherical. The cylindrical wave is emitted by a line source parallel to the edge, and the spherical wave is emitted by a point source (in the acoustic case) or by a Hertz dipole (in the electromagnetic case) parallel to the edge. The plane wave excitation is the limiting case if the source is taken to infinity.

Sommerfeld [47] developed the first rigorous solution for the diffraction of plane waves by a perfectly conducting half-plane. He used the concept of Riemann surfaces to deduce an integral solution of the problem in terms of Fresnel's integral. The extension of the approach to the three-dimensional case was accomplished by Sommerfeld in the case of potential theory [48]. He also derived the solution for a wedge of angle $(\frac{m\pi}{n})$, where m and n are integers, using a Riemann surface of m sheets [49]. Sommerfeld [50] later extended the solution to arbitrary wedge angles.

Carslaw [51] extended Sommerfeld's approach to cylindrical and spherical wave incidence as well as the three-dimensional plane wave diffraction by a half-plane [52]. The solution of the problem of diffraction of plane, cylindrical and spherical waves by a conducting wedge of arbitrary angle is due to Macdonald [53] who expanded the wave functions as a series of Bessel and trigonometric functions. Carslaw [54] rederived these results using contour integration. Wiegrefe [55] gave a mathematical analysis of the many-valued solutions of the wave equation and derived another integral solution to the problem. Starting from the series solution of the diffraction problem of cylindrical waves by a wedge and using an integral representation for Bessel functions, Macdonald [56] derived an integral solution similar to Wiegrefe's [55]. Another integral solution was presented by Carslaw [57]. His results agree with those of Macdonald [56]. Several integral forms for the solution of spherical wave diffraction were derived by Bromwich [58], Hanson [59] and Nomura [60, 61]. Following Bromwich's approach and using a generalization of the method of images, Herglotz [62] treated the problem of diffraction of waves by a wedge. Series as well as integral representations of the field for this problem were also given by Tuzhilin [63] using an integral approach.

Kontorovich and Lebedev [64] established the solution of plane wave diffraction by a half-plane by means of an

integral transform technique. This technique was later used by Jones [4, pp. 608-612] to treat the problem of plane, cylindrical and spherical wave diffraction by a wedge. Garnir [65] used the Lebedev transform to derive an integral solution for cylindrical wave excitation. The same approach was used by Oberhettinger [66, 67] who also obtained the results for plane wave and spherical wave excitation. Felsen [68] gave an analysis of the wedge diffraction problem in terms of spherical co-ordinates using Green's function technique. Williams [69] proposed a unified approach to the solution of a class of problems involving wedge surfaces. The solution was expressed as an integral superposition of plane waves of complex frequency such that the problem reduces to the solution of difference equations. He re-derived Oberhettinger's solution [66] for plane wave diffraction by a wedge. Using a similar approach, Faulkner [70] derived the solution for cylindrical and spherical wave incidence as an integral superposition of cylindrical and spherical waves, respectively. The problem was then reduced to Laplace's equation and the final solution was identical to that of Oberhettinger [66].

The two series solutions obtained by Macdonald [53] and Tuzhilin [63] are rapidly convergent if either the source or field point is near the edge. The computational effort increases considerably in the far field as has been indicated by Wait and Jackson [71] for plane wave incidence. In such

cases the integral solutions are used in order to derive asymptotic expressions for the field. The merit of the integral representation, as indicated by Harrington [72, p. 125], is that since all elements in the integration do not contribute equally, a good estimate for the integral may be obtained from the dominant contributions to the integrand.

The asymptotic evaluation of fields for the wedge diffraction problem has been considered by many investigators. Jackson [73] expressed the far field, for plane wave incidence, in terms of Fresnel's integral. Rieche [74] gave an asymptotic formula for the right angle wedge for the same excitation, while Wiegrefe [55] dealt with a more general wedge angle. Sommerfeld [50] treated the latter problem but his expression fails to give the proper behavior in the neighborhood of the boundaries of geometrical optics. Hanson [59] gave an asymptotic expression for the far field in terms of Fresnel's integral. In 1938, Pauli [43] gave the first satisfactory expansion of the solution for plane wave incidence, applying a modification of the method of steepest descents. While the leading term of his expansion is a Fresnel integral, the higher-order terms are confluent hypergeometric functions. This expansion was studied further by Ott [75] and Clemmow [76]. Oberhettinger [77] applied Watson's Lemma to derive another expression with the half-plane solution (in terms of

Fresnel's integral) as the leading term. The higher order terms were expanded as a series in inverse powers of the distance from the edge. The coefficients of this series are trigonometric functions of the wedge angle. Oberhettinger [78] showed that his expansion could also be derived by an application of Van der Waerden's modified method of steepest descents [79]. Hutchins and Kouyoumjian [80] generalized Pauli's expansion so that it could be applied to wedges of exterior angle less than 180°.

An asymptotic expression for spherical wave excitation was obtained by Whipple [95] in terms of Fresnel's integral. Nomura [60] also derived an integral solution for this excitation and used the saddle point method to express the final result in terms of Fresnel's integral. The analogous case, in which the field is due to a dipole whose axis is parallel to the edge of the wedge, was treated by Wait [81].

The asymptotic diffraction of cylindrical waves by a wedge was treated by Rudduck [21] who employed the principle of reciprocity together with the plane wave solution. Other expressions were suggested by Dybdal [82] and by Tsai and Rudduck [83] through the generalization of known formulas for the half-plane case. Recently, Lewin [46] treated the problem of diffraction of an H-polarized cylindrical wave in a more direct manner with emphasis on the shadow region.

Asymptotic diffraction of waves by conducting wedges was treated by Felsen and Marcuwitz [84] and by Tuzhilin [63]. Far field diffraction expressions for plane and cylindrical waves were derived by Ufimtsev [85]. His method depends on reducing the elliptic wave equation to a parabolic equation and then obtaining an integral solution which can be evaluated asymptotically.

As pointed out by Hutchins [86], the asymptotic expressions of Pauli and Oberhettinger, for plane wave excitation, are the most commonly used in the ray optical solution of diffraction problems where edges are encountered. Hutchins also discussed the inadequacies in these expansions, such as the restriction that the exterior wedge angle be greater than 180°, and the inaccuracy of the expansions in certain cases.

The main objective of this chapter is to obtain accurate asymptotic expressions for the field diffracted by a perfectly conducting wedge due to plane as well as cylindrical and spherical wave excitation. The advantage of such expressions is to extend the range of accuracy of ray optical solutions of diffraction problems of complex bodies, consisting of wedge-like structures, from high to lower frequencies. In particular, these expressions lead to near field edge-edge interaction terms and field expansions along shadow boundaries which are more reliable than those based on the usual diffraction coefficient [3].

In this chapter the problem of diffraction of plane, cylindrical and spherical waves by a perfectly conducting wedge is treated using a unified approach. Starting from the wave equation, the series solution for the diffraction of cylindrical waves by a perfectly conducting wedge is obtained. By using an integral expression for the product of Bessel functions, the solution is represented as the sum of geometrical optics terms and diffraction integrals. The corresponding results for plane wave incidence are deduced by letting the line source go to infinity. The solution for spherical wave incidence is obtained from the cylindrical wave case using an integral relation between the expressions for the two types of excitations. The saddle point method is then used to evaluate asymptotically the diffraction integrals encountered. The results are compared with available exact and approximate solutions.

2.2 Derivation of the Exact Solutions for Cylindrical, Plane and Spherical Wave Excitations

2.2.1 *Cylindrical Wave Excitation*

Consider a perfectly conducting wedge of exterior angle α illuminated by a line source at (r_0,ϕ_0) as shown in Fig. 2.1. Since the problem of diffraction is two-dimensional, the scalar field U^c satisfies the Helmholtz equation and corresponds to the magnitude of the electric field (E) or magnetic field (H), depending on whether the incident electric or magnetic vector is parallel to the edge, respectively. The analysis is presented in cylindrical co-ordinates (r,ϕ,z) where the z axis coincides with the edge of the wedge. The $e^{j\omega t}$ time dependence, where ω denotes the angular frequency, is suppressed.

The scalar function U^c should satisfy the following requirements:

(a) the wave equation

$$\nabla^2 U^c + k^2 U^c = -4 \frac{j}{r_0} \delta(r - r_0)\ \delta(\phi - \phi_0) \qquad (2.2.1)$$

which is a result of Maxwell's equations. Here ∇^2 is the two-dimensional Laplacian operator, δ is Dirac's function, $k^2 = \omega^2 \mu_0 \varepsilon_0$ and μ_0 and ε_0 denote the permeability and permittivity of free space, respectively. The superscript c denotes cylindrical wave excitation.

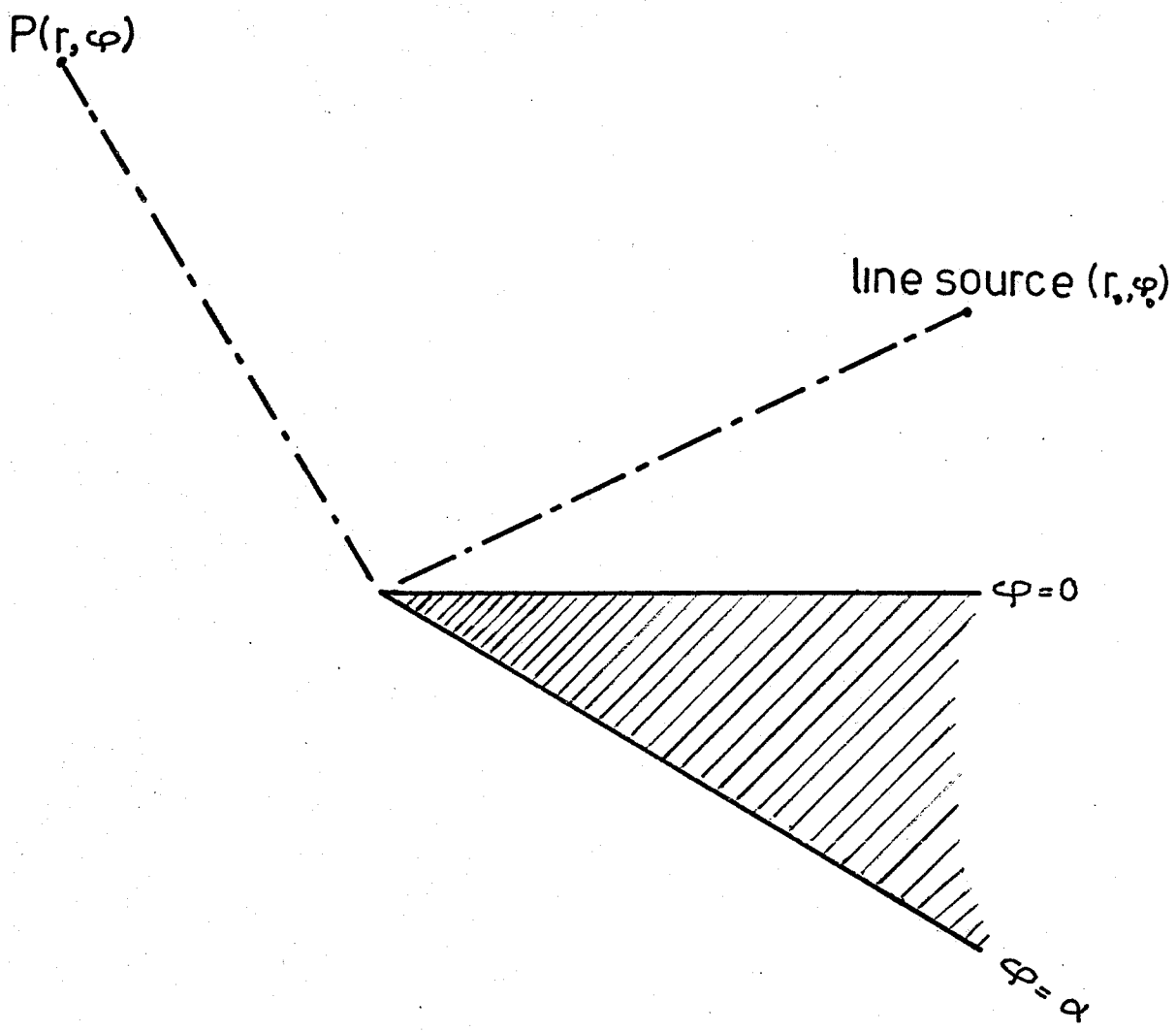

Fig. 2.1. Schematic diagram of a perfectly conducting wedge with line source excitation.

(b) the edge condition which is necessary for a unique solution [87, 88].

(c) the radiation condition.

(d) U^c or $\frac{\partial U^c}{\partial \phi}$ vanishes at $\phi = 0, \alpha$ so as to satisfy the Dirichlet or Neumann boundary condition, respectively.

In order to use a unified approach for both boundary conditions, a solution $U^c_\alpha(\phi)$ is obtained satisfying the boundary conditions [65]*

$$U^c_\alpha(0) = U^c_\alpha(\alpha) \tag{2.2.2}$$

$$\left.\frac{\partial U^c_\alpha(\phi)}{\partial \phi}\right|_{\phi=0} = \left.\frac{\partial U^c_\alpha(\phi)}{\partial \phi}\right|_{\phi=\alpha} \tag{2.2.3}$$

In terms of the auxiliary solution $U^c_\alpha(\phi)$, it may be shown that the solution for the Dirichlet condition is**

$$U^c = U^c_{2\alpha}(\phi) - U^c_{2\alpha}(2\alpha - \phi) \tag{2.2.4}$$

while the solution for the Neumann condition is

$$U^c = U^c_{2\alpha}(\phi) + U^c_{2\alpha}(2\alpha - \phi) \tag{2.2.5}$$

Such formulation has the advantage that it can be used in cases having the Dirichlet condition on one side and

---

* The final solution is shown later to satisfy all the boundary conditions in spite of the fact that the boundary conditions (2.2.2) and (2.2.3) have no physical interpretation.

** Equations (2.2.4) and (2.2.5) follow from (2.2.2) and (2.2.3), respectively.

the Neumann condition on the other. For example, when the function U^C vanishes on the surface $\phi = 0$ and its derivative vanishes for $\phi = \alpha$, the solution is

$$U^C = U^C_{4\alpha}(\phi) + U^C_{4\alpha}(2\alpha - \phi) - U^C_{4\alpha}(2\alpha + \phi) - U^C_{4\alpha}(4\alpha - \phi) \quad (2.2.6)$$

Using separation of variables, the solution for the two-dimensional wave equation has the form [72, p. 231]

$$U^C_\alpha(\phi) = \sum_\mu J_\mu (kr_<) H^{(2)}_\mu (kr_>) \{a_\mu \sin \mu\phi + b_\mu \cos \mu\phi\} \quad (2.2.7)$$

where

$$r_{\lessgtr} = \begin{cases} r & \text{if } r \lessgtr r_0 \\ r_0 & \text{if } r \gtrless r_0 \end{cases}$$

while μ is a separation constant. Applying the boundary conditions on $U^C_\alpha(\phi)$ we obtain

$$b_\mu = a_\mu \sin \mu\alpha + b_\mu \cos \mu\alpha$$

and

$$a_\mu = a_\mu \cos \mu\alpha - b_\mu \sin \mu\alpha$$

The non-trivial solution of these two equations for a_μ and b_μ requires that the determinant of the coefficients be equal to zero. Thus

$$\sin^2 \mu\alpha + (1 - \cos \mu\alpha)^2 = 0$$

or

$$\cos \mu\alpha = 1$$

from which

$$\mu = \frac{2n\pi}{\alpha} \; ; \quad n = 0, 1, 2, \ldots$$

The negative values of n are excluded, since for a general value of α, μ is non-integer and the Bessel function of non-integer negative order is singular for zero arguments, which violates the edge condition [88].

The discontinuity at (r_0, ϕ_0) implies that

$$\sum_{n=0}^{\infty} k \{a_\mu \sin \mu\phi + b_\mu \cos \mu\phi\} \{J_\mu(kr_0) \acute{H}_\mu^{(2)}(kr_0) - \acute{J}_\mu(kr_0) H_\mu^{(2)}(kr_0)\} = 4 \frac{j}{r} \delta(\phi - \phi_0) \qquad (2.2.8)$$

Using the Wronskian for Bessel functions [89, p. 360], equation (2.2.8) is reduced to

$$\sum_{n=0}^{\infty} \{a_\mu \sin \mu\phi + b_\mu \cos \mu\phi\} = 2\pi \, \delta(\phi - \phi_0)$$

giving

$$\left.\begin{aligned} a_\mu &= \varepsilon_n \frac{2\pi}{\alpha} \sin \mu\phi_0 \\ b_\mu &= \varepsilon_n \frac{2\pi}{\alpha} \cos \mu\phi_0 \end{aligned}\right\} \quad \text{where } \varepsilon_n = \begin{cases} 1 & n = 0 \\ 2 & n = 1,2, \ldots \end{cases}$$

Thus,

$$U_{\alpha}^{c}(\phi) = \sum_{n=0}^{\infty} \varepsilon_n \frac{2\pi}{\alpha} \cos \mu(\phi - \phi_0) J_{\nu}(kr_{<}) H_{\nu}^{(2)}(kr_{>})$$

Using (2.2.4) and (2.2.5), the solution (U^c) is given by

$$U^{c} = \frac{\pi}{\alpha} \sum_{n=0}^{\infty} \varepsilon_n J\nu(kr_{<}) H_{\nu}^{(2)}(kr_{>})\{\cos \nu(\phi - \phi_0) \mp \cos \nu(\phi + \phi_0)\} \tag{2.2.9}$$

where $\nu = \frac{n\pi}{\alpha}$ and the upper and lower signs apply for the E and H polarizations, respectively. This solution satisfies all the requirements, including the reciprocity condition which implies that

$$U^{c}(r,\phi;r_0,\phi_0) = U^{c}(r_0,\phi_0;r,\phi)$$

Furthermore, since $J_{\mu}(z) \sim \frac{1}{\sqrt{2\pi\mu}} (\frac{ez}{2\mu})^{\mu}$ when $\mu >> z$ [89, p. 365] the series converges rapidly and may be used for numerical evaluation when either the source or observation point is located near the edge. To obtain an expression which converges rapidly for other cases, an integral representation of the solution is derived next.

From the series solution, equation (2.2.9), different integral representations of the field can be deduced by employing different integral forms for the product of Bessel functions. Thus, many such representations have been obtained by many authors, e.g. Oberhettinger [67], Hutchins [86] and Lewin [46]. The integral form for the product of

Bessel functions employed by Oberhettinger [67] is used in the next analysis. It should be noted, however, that the derivation of this form as well as the subsequent analysis are different from Oberhettinger's.

Letting $\gamma = jk$ and using the following relations between Bessel and Macdonald functions*[89, p. 375]

$$J_\nu(-jz) = e^{-j\nu\frac{\pi}{2}} I_\nu(z)$$

and

$$H_\nu^{(2)}(-jz) = \frac{2j}{\pi} e^{j\nu\frac{\pi}{2}} K_\nu(z)$$

the equation for the field, for $r > r_0$, is reduced to

$$U^c = \frac{2j}{\alpha} \sum_{n=0}^{\infty} \varepsilon_n I_\nu(\gamma r_0) K_\nu(\gamma r)\{\cos \nu(\phi - \phi_0) \mp \cos \nu(\phi + \phi_0)\}$$

$$= S^c(|\phi - \phi_0|) \mp S^c(|\phi + \phi_0|) \qquad (2.2.10)$$

which implies that

$$S^c(\theta) = \frac{2j}{\alpha} \sum_{n=0}^{\infty} \varepsilon_n I_\nu(\gamma r_0) K_\nu(\gamma r) \cos \nu\theta \qquad (2.2.11)$$

Using the integral relation (A.6) for the product $I_\nu(\gamma r_0) K_\nu(\gamma r)$, $S^c(\theta)$ is then given by

---

* The advantage of using Macdonald functions is that the solution can be written in terms of integrals on the real axis as the following development shows.

$$S^c(\theta) = \frac{2j}{\alpha\pi} \sum_{n=0}^{\infty} \varepsilon_n \cos \nu\theta \left\{ \int_0^{\pi} \cos \nu x \, K_0[\gamma D(x)]dx \right.$$

$$\left. - \sin \nu\pi \int_0^{\infty} e^{-\nu x} K_0[\nu(r^2 + r_0^2 + 2rr_0 \cosh x)^{\frac{1}{2}}] \, dx \right\}$$

(2.2.12)

where $D^2(x) = r^2 + r_0^2 - 2rr_0 \cos x$.

Denoting the first and second summations in (2.2.12) by S_1^c and S_2^c, respectively, we have

$$S_1^c = \frac{j}{\alpha\pi} \int_{-\pi}^{\pi} K_0[\gamma D(x)] \sum_{n=0}^{\infty} \varepsilon_n \cos \nu\theta \cos \nu x \, dx$$

$$= \frac{j}{\alpha\pi} \int_{-\pi}^{\pi} K_0[\gamma D(x)] \sum_{n=-\infty}^{\infty} e^{j\nu(x-\theta)} \, dx \qquad (2.2.13)$$

since $K_0[\gamma D(x)]$ is an even function of x. Since a periodic delta function $\sum_{-\infty}^{\infty} \delta[x - (\theta + 2\alpha N)]$, where N is an integer, can be expanded in a Fourier series in the form

$$\sum_{-\infty}^{\infty} \delta[x - (\theta + 2\alpha N)] = \frac{1}{2\alpha} \sum_{-\infty}^{\infty} e^{j\frac{n\pi}{\alpha}(x-\theta)} \qquad (2.2.14)$$

S_1^c is thus given by [90, p. 742]

$$S_1^c = \frac{2j}{\pi} \int_{-\pi}^{\pi} K_0[\gamma D(x)] \sum_{-\infty}^{\infty} \delta[x - (\theta + 2\alpha N)] \, dx$$

$$= \frac{2j}{\pi} \sum_{N=N_1}^{N=N_2} K_0[\gamma D(\theta + 2\alpha N)] \, H(\pi - |\theta + 2\alpha N|) \qquad (2.2.15)$$

Here, N_1 and N_2 are the lowest and highest integers satisfying the relation $\pi \geq \theta + 2\alpha N \geq -\pi$, and

$$H(x) = \begin{cases} 1 & x > 0 \\ \frac{1}{2} & x = 0 \\ 0 & x < 0 \end{cases} \qquad (2.2.16)$$

Substituting $\gamma = jk$ in (2.2.15), S_1^c is then given by

$$S_1^c = \sum_{N_1}^{N_2} H_0^{(2)} [k\, D(\theta + 2\alpha N)]\; H(\pi - |\theta + 2\alpha N|) \qquad (2.2.17)$$

which represents the geometrical optics term, i.e. the sum of the field on incident plus singly and multiply reflected rays.

By interchanging the order of summation and integration and evaluating the sum [91, p. 40], the expression for S_2^c is given by

$$S_2^c = -\frac{2j}{\alpha\pi} \int_0^\infty K_0[\gamma(r^2 + r_0^2 + 2rr_0 \cosh x)^{\frac{1}{2}}] \{\sum_{n=0}^{\infty} \varepsilon_n e^{-\nu x} \sin \nu\pi \cos \nu\theta\}\, dx$$

$$= -\frac{j}{\alpha\pi} \int_0^\infty K_0[\gamma(r^2 + r_0^2 + 2rr_0 \cosh x)^{\frac{1}{2}}] \{\sum_{n=0}^{\infty} \varepsilon_n e^{-\nu x} [\sin \nu(\pi-\theta) + \sin \nu(\pi+\theta)]\}\, dx$$

$$= -\frac{j}{\alpha\pi} \int_0^\infty K_0[\gamma(r^2 + r_0^2 + 2rr_0 \cosh x)^{\frac{1}{2}}]\; \Lambda(\theta,x)\, dx \qquad (2.2.18)$$

where

$$\Lambda(\theta,x) = \frac{\sin \frac{\pi}{\alpha}(\pi-\theta)}{\cosh \frac{\pi}{\alpha}x - \cos \frac{\pi}{\alpha}(\pi-\theta)} + \frac{\sin \frac{\pi}{\alpha}(\pi+\theta)}{\cosh \frac{\pi}{\alpha}x - \cos \frac{\pi}{\alpha}(\pi+\theta)} \qquad (2.2.19)$$

S_2^c represents a diffraction term which vanishes when the wedge angle is a submultiple of π, as expected.*

If α is taken to be greater than $\pi + \phi_0$, it is apparent that the incident wave, being zero in the shadow region ($\pi + \phi_0 < \phi < \alpha$), is discontinuous at the shadow boundary. Similarly, the singly reflected geometrical optics wave consists of a cylindrical wave in the region ($0 < \phi < \pi - \phi_0$) and is zero in the region ($\pi - \phi_0 < \phi < \alpha$). The two regions are separated by the shadow boundary at $\phi = \pi - \phi_0$. The same analysis holds for the multiply reflected rays for $\alpha < \pi + \phi_0$. The diffracted wave combines with the associated geometrical optics wave to eliminate the discontinuity at the corresponding shadow boundary as will be shown later.

It is to be noted that equations (2.2.15) and (2.2.18) are valid for all values of r and r_0 as may be realized from the symmetry of the expressions with respect to r and r_0.

2.2.2 *Plane Wave Excitation*

(a) The two-dimensional case:

The plane wave diffraction case may be easily deduced from the previous cylindrical wave solution by using the large argument asymptotic form of the Hankel function [89, p. 364], that is

$$H_n^{(2)}(z) \sim \sqrt{\frac{2}{\pi z}}\, e^{-j\left[z - \frac{\pi}{2}(n+\frac{1}{2})\right]} \qquad (2.2.20)$$

---

* since the field in this case is due to a finite number of images (geometrical optics field).

Thus, the total field due to the diffraction of a plane wave $e^{jkr\cos(\phi-\phi_0)}$ incident at an angle ϕ_0 with respect to the surface ($\phi = 0$) of a perfectly conducting wedge is given by

$$U^p = S^p\,(|\phi - \phi_0|) \mp S^p\,(|\phi + \phi_0|) \qquad (2.2.21)$$

where the superscript p denotes plane wave excitation and as in the cylindrical wave case, the negative sign applies for the Dirichlet condition and the positive sign for the Neumann condition, and

$$S^p(\theta) = S_1^p + S_2^p \qquad (2.2.22)$$

where

$$S_1^p = \sum_{N_1}^{N_2} e^{jkr\cos(\theta+2\alpha N)}\; H\,\{\pi - |\theta+2\alpha N|\} \qquad (2.2.23)$$

$$S_2^p = \frac{-1}{2\alpha} \int_0^\infty e^{-jkr\cosh x}\, \Lambda(\theta,x)\, dx \qquad (2.2.24)$$

(b) The three-dimensional case:

The incident wave in this case is represented by $e^{jk\{r\sin\psi_0\cdot\cos(\phi-\phi_0)+z\cos\psi_0\}}$ where ψ_0 is the angle between the direction of incidence and the z axis and ϕ_0 is the angle between the projection of the direction of propagation on the plane $z = 0$ and the line $\phi = 0$.

Due to the infinite extension of the edge, the z-dependence of the total field remains the same as the

incident field and the result for the two-dimensional case can be extended to the present case if k is replaced by $k \sin\psi_0$ and the field is multiplied by the factor $e^{jk\cos\psi_0 z}$.

2.2.3 *Spherical Wave Excitation*

The wedge in this case is excited by a Hertz dipole whose axis is parallel to the edge. The solution for the Hertz vector (π_z) can be formulated from the cylindrical wave case by using the formula [91, p. 736]

$$\frac{e^{-\gamma(r^2+z^2)^{\frac{1}{2}}}}{(r^2+z^2)^{\frac{1}{2}}} = \frac{2}{\pi}\int_0^\infty K_0\{(\gamma^2 + \nu^2)^{\frac{1}{2}} r\}\cos z\nu \, d\nu \quad (2.2.25)$$

i.e. the field is obtained from (2.2.15) and (2.2.18) by substituting $(\gamma^2 + \nu^2)^{\frac{1}{2}}$ for γ, multiplying by cos $z\nu$ and integrating with respect to ν from 0 to ∞.* The resulting expression consists of geometrical optics term (S_1^s) and diffraction term (S_2^s) which are given explicitly by

$$S_1^s = \sum_{N_1}^{N_2} \frac{e^{-jkY_N}}{Y_N} H(\pi - |\theta+2\alpha N|) \quad (2.2.26)$$

and

$$S_2^s = \frac{-1}{2\alpha}\int_0^\infty \frac{e^{-jkY}}{Y} \Lambda(\theta,x)\, dx \quad (2.2.27)$$

where the superscript s denotes spherical wave excitation,

---

* Similar procedures were employed by Clemmow [92] and Oberhettinger [66].

and

$$Y_N = \{r^2 + r_0^2 - 2rr_0\cos(\theta+2\alpha N) + (z-z_0)^2\}^{\frac{1}{2}}$$

$$Y = \{r^2 + r_0^2 + 2rr_0\cosh x + (z-z_0)^2\}^{\frac{1}{2}}$$

and (r_0,ϕ_0,z_0) are the cylindrical co-ordinates of the source.

Applying the inverse cosine Fourier transform to (2.2.25), the relations (2.2.15) and (2.2.18) for cylindrical wave excitation in terms of the spherical wave solution are obtained. This is a convenient method to express the solution for the former excitation if the solution for spherical excitation is known. Furthermore, the solution for plane wave excitation can be obtained from both the cylindrical and spherical wave cases by letting $kr_0 \to \infty$.

2.3 Asymptotic Evaluation of the Diffracted Field

In this section, we derive asymptotic expressions for the diffracted field due to the three types of excitation. The saddle point method is used to express the diffraction integral S_2 in terms of Fresnel's integral. The accuracy of these expressions is established by comparison with previous approximate results as well as available exact solutions.

2.3.1 *Plane Wave Excitation*

(a) Two-dimensional case:

In this case, the diffraction integral S_2^p may be expressed in the form

$$S_2^p = \frac{-1}{2\alpha} \int_0^\infty e^{-jkr\cosh x} \Lambda(\theta,x)\, dx$$

$$= I^p(\pi-\theta,kr) + I^p(\pi+\theta,kr) \qquad (2.3.1)$$

where $\theta = |\phi \mp \phi_0|$ and

$$I^p(\delta,kr) = -\frac{\sin\frac{\pi\delta}{\alpha}}{2\alpha} \int_0^\infty \frac{e^{-jkr\cosh x}}{\cosh\frac{\pi x}{\alpha} - \cos\frac{\pi\delta}{\alpha}}\, dx \qquad (2.3.2)$$

The plane wave diffraction integral $I^p(\delta,kr)$ was evaluated asymptotically by Oberhettinger [77] using Watson's Lemma. The leading term of his expression is the same as that for the half-plane solution, while the higher order terms represent the effect of the angle of the wedge. A recursion

relation for the various coefficients of the expansion was reported elsewhere [93].

A more convenient evaluation of $I^p(\delta,kr)$ is obtained next by using the saddle point method [4, p. 449]. For large kr (compared to unity), the exponent in the integrand of (2.3.2) is large and therefore the integrand oscillates rapidly. By the principle of stationary phase, the only important contributions are in the neighborhood of the saddle point where the exponential term makes its maximum contribution, i.e. at sinh x = 0 or x = 0. Expanding the cosh terms in the vicinity of this point and retaining only the first two terms, we obtain

$$I^p(\delta,kr) \simeq -\frac{\sin\frac{\pi\delta}{\alpha}}{2\alpha} e^{-jkr} \int_0^\infty \frac{e^{-jkr\frac{x^2}{2}}}{1 + \frac{1}{2}(\frac{\pi x}{\alpha})^2 - \cos\frac{\pi\delta}{\alpha}} dx$$

$$\simeq -\frac{\alpha}{\pi^2} \sin\frac{\pi\delta}{\alpha} e^{-jkr} \int_0^\infty \frac{e^{-jkr\frac{x^2}{2}}}{x^2 + (\frac{2\alpha}{\pi}\sin\frac{\pi\delta}{2\alpha})^2} dx \quad (2.3.3)$$

and the new integral on the right hand side can be evaluated in closed form [94, p. 568] since

$$\int_0^\infty \frac{e^{-j\alpha x^2}}{x^2 + \beta^2} dx = \frac{\sqrt{\pi}}{|\beta|} e^{j\alpha\beta^2 + j\frac{\pi}{4}} F(|\beta|\sqrt{\alpha}) \quad (2.3.4)$$

Hence

$$I^p(\delta,kr) \simeq -\cos T \operatorname{sgn} T \frac{e^{-jkr}}{\sqrt{\pi}} e^{j\varepsilon^2 + j\frac{\pi}{4}} F(\varepsilon) \quad (2.3.5)$$

where $T = \frac{\pi\delta}{2\alpha}$, $\varepsilon = \frac{\alpha}{\pi}|\sin T|\sqrt{2kr}$ and Fresnel's integral $F(\varepsilon)$ is defined by

$$F(\varepsilon) = \int_{\varepsilon}^{\infty} e^{-jt^2}\, dt \tag{2.3.6}$$

Since the shadow boundaries, for $\alpha > \pi + \phi_0$, corresponds to $\delta = 0$ the continuity of the solution at these boundaries requires the evaluation of $\lim_{\delta\to 0} I^p(\delta,kr)$. It is apparent from the definition (2.3.2) that the integral equals zero except in the vicinity of $x = 0$ which is the saddle point, and subsequently may be used for this evaluation. At $\delta = 0$ we have

$$F(0) = \int_{0}^{\infty} e^{-jt^2}\, dt = \frac{\sqrt{\pi}}{2} e^{-j\frac{\pi}{4}}$$

Hence

$$\lim_{\delta\to\pm 0} I^p(\delta,kr) = -\frac{e^{-jkr}}{2} \lim_{\delta\to\pm 0} \operatorname{sgn}\delta \tag{2.3.7}$$

As the geometrical optics terms are halved at the shadow boundaries, the definition of sgn δ is taken such that

$$\lim_{\delta\to+0} \operatorname{sgn}\delta = 0 \quad \text{and} \quad \lim_{\delta\to-0} \operatorname{sgn}\delta = -1 \tag{2.3.8}$$

which ensures the continuity at the shadow boundaries. On the other hand, if $H(x)$ is defined by

$$H(x) = \begin{cases} 1 & x \geq 0 \\ 0 & x < 0 \end{cases} \tag{2.3.9}$$

the above limit becomes

$$\lim_{\delta \to \pm 0} \operatorname{sgn} \delta = \pm 1 \tag{2.3.10}$$

The latter definition is used in Chapter 3.

It is to be noted that for small values of δ, the integral $I^p(\delta,kr)$ has the asymptotic value

$$I^p(\delta,kr) \simeq - \operatorname{sgn} \delta \frac{e^{-jkr}}{\sqrt{\pi}} e^{j\delta^2 \frac{kr}{2}} + j\frac{\pi}{4} F(|\delta|\{\frac{kr}{2}\}^{\frac{1}{2}}) \tag{2.3.11}$$

which is independent of α.

If $\theta \to (\pm\pi+2N\alpha)$ and N is assumed an integer, the same analysis holds with δ replaced by $\delta+2N\alpha$ in (2.3.2) and the consequent equations [43].

For the case of a half-plane ($\alpha = 2\pi$), the same technique can be used to evaluate (2.3.1). In this case S_2^p is given by

$$S_2^p = - \frac{1}{4\pi} \int_0^\infty e^{-jkr\cosh x} \Lambda(\theta,x)\, dx \tag{2.3.12}$$

where, for $\alpha = 2\pi$,

$$\Lambda(\theta,x) = \frac{\sin(\frac{\pi-\theta}{2})}{\cosh(\frac{x}{2}) - \cos(\frac{\pi-\theta}{2})} + \frac{\sin(\frac{\pi+\theta}{2})}{\cosh(\frac{x}{2}) - \cos(\frac{\pi+\theta}{2})}$$

$$= \cos\frac{\theta}{2} \frac{2\cosh\frac{x}{2}}{(\cosh\frac{x}{2} - \sin\frac{\theta}{2})(\cosh\frac{x}{2} + \sin\frac{\theta}{2})}$$

$$= 4 \cos \frac{\theta}{2} \frac{\cosh \frac{x}{2}}{(\cosh x - 1) + 2 \cos^2 \frac{\theta}{2}} \qquad (2.3.13)$$

For large kr, the saddle point method is used to evaluate S_2^p. As before, the saddle point is at x = 0 in the neighborhood of which we have

$$\Lambda(\theta,x) \sim \frac{8 \cos \frac{\theta}{2}}{x^2 + (2 \cos \frac{\theta}{2})^2} \qquad (2.3.14)$$

and

$$S_2^p = - \frac{2 \cos \frac{\theta}{2}}{\pi} e^{-jkr} \int_0^\infty \frac{e^{-j\frac{kr}{2}x^2}}{x^2 + (2 \cos \frac{\theta}{2})^2} dx \qquad (2.3.15)$$

As previously shown, this integeral may be evaluated in terms of Fresnel's integral, that is

$$S_2^p = (\mp) \frac{e^{jkr\cos\theta + j\frac{\pi}{4}}}{\sqrt{\pi}} F(|\cos \frac{\theta}{2}| \{2kr\}^{\frac{1}{2}}) \qquad (2.3.16)$$

where the upper sign holds for $\theta < \pi$ and the lower sign for $\theta > \pi$, and the definitions (2.3.9) and (2.3.10) are used. Equation (2.3.16) is in agreement with Sommerfeld's solution [43, equation 14] obtained by a different approach.

(b) Three-dimensional case:

In this case the diffraction integral is denoted by $I^p(\delta,kr,kz)$ whose asymptotic form is given by

$$I^{p}(\delta,kr,kz) \simeq - \cos T \operatorname{sgn} T \frac{e^{-jk\sin\psi_0 r+jk\cos\psi_0 z}}{\sqrt{\pi}} e^{j\varepsilon^2+j\frac{\pi}{4}} F(\varepsilon) \tag{2.3.17}$$

where

$$\varepsilon = \frac{\alpha}{\pi} |\sin T| (2kr\sin\psi_0)^{\frac{1}{2}}$$

The similarity previously indicated between the two-dimensional and three-dimensional plane wave excitation was utilized in writing (2.3.17) with the aid of (2.3.5).

2.3.2 *Cylindrical Wave Excitation*

In this case, the cylindrical wave diffraction integral may be written as

$$I^{c}(\delta,kr,kr_0) = - \frac{\sin\frac{\pi\delta}{\alpha}}{2\alpha} \int_0^{\infty} \frac{H_0^{(2)}(k\sqrt{r^2+r_0^2+2rr_0\cosh x})}{\cosh\frac{\pi x}{\alpha} - \cos\frac{\pi\delta}{\alpha}} dx \tag{2.3.18}$$

using the asymptotic expansion of the Hankel function for large argument [89, p. 364], this integral reduces to

$$I^{c}(\delta,kr,kr_0) \simeq - \{\frac{\sin\frac{\pi\delta}{\alpha}}{2\alpha} \sqrt{\frac{2}{\pi}}\} \{\int_0^{\infty} \frac{e^{-jk\sqrt{r^2+r_0^2+2rr_0\cosh x}+ j\frac{\pi}{4}}}{\sqrt{k}\{r^2+r_0^2+2rr_0\cosh x\}^{\frac{1}{2}}} \frac{dx}{\cosh\frac{\pi x}{\alpha} - \cos\frac{\pi\delta}{\alpha}}\} \tag{2.3.19}$$

For large $k\sqrt{rr_0}$, the saddle point technique can be applied as shown previously. Again, the saddle point is at $x = 0$ in which

vicinity

$$k(r^2+r_0^2+2rr_0\cosh x)^{\frac{1}{2}} \simeq kR + k\frac{rr_0}{2R}x^2 \qquad (2.3.20)$$

where $R = r + r_0$. Expanding the cosh terms in the vicinity of $x = 0$ and evaluating the resultant integral as before, we obtain

$$I^c(\delta,kr,kr_0) \simeq -\frac{\sin\frac{\pi\delta}{\alpha}}{2\alpha}\left(\frac{2}{\pi}\right)^{\frac{1}{2}}\int_0^\infty \frac{e^{-jkR-jk\frac{rr_0}{2R}x^2}}{(kR\{1+\frac{rr_0}{2R^2}x^2\})^{\frac{1}{2}}}\frac{dx}{1+\frac{1}{2}(\frac{\pi x}{\alpha})^2-\cos\frac{\pi\delta}{\alpha}}$$

$$\simeq -\frac{\sin\frac{\pi\delta}{\alpha}}{\pi^2}\left(\frac{2}{\pi}\right)^{\frac{1}{2}}\frac{e^{-jkR}}{\sqrt{kR}}\int_0^\infty \frac{e^{-jk\frac{rr_0}{2R}x^2}}{\Delta x^2+(\frac{2\alpha}{\pi}\sin\frac{\pi\delta}{2\alpha})}dx$$

$$\simeq -\frac{\sqrt{2}}{\pi}\cos T\ \mathrm{sgn}\ T\ \frac{e^{-jkR}}{\sqrt{k\Delta R}}e^{j\beta^2+j\frac{\pi}{4}}F(\beta) \qquad (2.3.21)$$

where $\Delta = 1+\frac{rr_0}{4R^2}(\frac{2\alpha}{\pi}\sin T)^2$, and $\beta = \frac{\alpha}{\pi}|\sin T|(2k\frac{rr_0}{\Delta R})^{\frac{1}{2}}$. This result agrees with Lewin's [46], who considered only the H-polarization case, if Δ equals unity. Δ is approximately unity when $r>>r_0$, $kr_0>>1$ or $r<<r_0$, $kr>>1$ and has a maximum value of two when $r = r_0$, $\alpha = 2\pi$ and $T = 0$.

The result for plane wave excitation may be obtained from (2.3.21) by letting kr_0 tend to infinity and taking the expression $(\frac{2}{\pi kr_0})^{\frac{1}{2}}e^{-jkr_0+j\frac{\pi}{4}}$ as unity since the incident cylindrical wave $H_0^{(2)}[k\{r^2+r_0^2-2rr_0\cos(\phi-\phi_0)\}^{\frac{1}{2}}]$ tends to $(\frac{2}{\pi kr_0})^{\frac{1}{2}}e^{-jkr_0+j\frac{\pi}{4}}\{e^{jkr\cos(\phi-\phi_0)}\}$ as kr_0 tends to infinity.

It is also interesting to note that by letting kr tend to infinity $I^c(\delta,kr,kr_0)$ tends to

$$\lim_{kr\to\infty} I^c(\delta,kr,kr_0) \simeq -\frac{\sqrt{2}}{\pi}\cos T \operatorname{sgn} T \frac{e^{-jkr}}{\sqrt{kr}} e^{-jkr_0+j\xi_0^2+j\frac{\pi}{2}} F(\xi_0)$$

$$\simeq + \{(\frac{2}{\pi kr})^{\frac{1}{2}} e^{-jkr+j\frac{\pi}{4}}\} I^p(\delta,kr_0) \qquad (2.3.22)$$

where $\xi_0 = \frac{\alpha}{\pi}|\sin T|\sqrt{2kr_0}$. Thus, the far field due to a line source can be deduced from that of the plane wave excitation by interchanging the co-ordinates of the field and source points and multiplying by $\{(\frac{2}{\pi kr})^{\frac{1}{2}} e^{-jkr+j\frac{\pi}{4}}\}$. This result is due to the reciprocity principle [72, p. 116] which will be employed in the next chapter.

As for the plane wave case, the asymptotic value of $I^c(\delta,kr,kr_0)$ is independent of α for small values of δ.

2.3.3 *Spherical Wave Excitation*

In this case the spherical diffraction integral is denoted by $I^s(\delta,kY)$ and takes the form

$$I^s(\delta,kY) = -\frac{\sin\frac{\pi\delta}{\alpha}}{2\alpha}\int_0^\infty \frac{e^{-jkY}}{Y}\frac{dx}{\cosh\frac{\pi x}{\alpha}-\cos\frac{\pi\delta}{\alpha}} \qquad (2.3.23)$$

Applying the saddle point technique as shown in section 2.3.2 we obtain

$$I^s(\delta,kY) \simeq -\frac{\cos T}{\{\pi\bar{\Delta}\}^{\frac{1}{2}}} \operatorname{sgn} T \frac{e^{-jk\bar{R}}}{\bar{R}} e^{j\xi^2+j\frac{\pi}{4}} F(\xi) \qquad (2.3.24)$$

where $\bar{\Delta} = 1 + \frac{rr_0}{2\bar{R}^2} (\frac{2\alpha}{\pi} \sin T)^2$, $\bar{R} = \{(r+r_0)^2 + (z-z_0)^2\}^{\frac{1}{2}}$

and $\xi = \frac{\alpha}{\pi} |\sin T| (2k\frac{rr_0}{\bar{\Delta}\bar{R}})^{\frac{1}{2}}$.

If $\bar{\Delta}$ is taken to be unity, this expression will become identical to that given by Whipple [95]. $\bar{\Delta}$ has a maximum value of three when $r = r_0$, $z = z_0$, $\alpha = 2\pi$ and $T = 0$ and is approximately unity when $r>>r_0$, $kr_0>>1$ or $r<<r_0$, $kr>>1$.

Again, the result for plane wave excitation may be deduced from (2.3.13) by letting kr_0 tend to infinity and $z = z_0$. Also, the expression $\frac{e^{-jkr_0}}{r_0}$ is taken as unity since as kr_0 tends to infinity the incident field $\frac{e^{-jkY_0}}{Y_0}$ tends to $\{\frac{e^{-jkr_0}}{r_0}\} e^{jkr\cos(\phi-\phi_0)}$ if $z = z_0$. As in the cylindrical wave case, if $kr\to\infty$ and $z = z_0$, $I^s(\delta,kY)$ tends to

$$\lim_{kr\to\infty} I^s(\delta,kY) \simeq - \frac{\cos T}{\sqrt{\pi}} \operatorname{sgn} T \frac{e^{-jkr}}{r} e^{-jkr_0+j\xi_0^2+j\frac{\pi}{4}} F(\xi_0)$$

$$\simeq \{\frac{e^{-jkr}}{r}\} I^p(\delta,kr_0) \qquad (2.3.25)$$

Thus, the far field due to spherical waves in the plane $z = z_0$, may be deduced from that of the plane wave excitation by interchanging co-ordinates of the field and source points and multiplying by $\{\frac{e^{-jkr}}{r}\}$.

As in the case of plane and cylindrical wave excitation, the asymptotic value for $I^s(\delta,kY)$ for the spherical wave case, for small values of δ, is independent of α.

For the case of diffraction by a half plane, the integral S_2^s has the form

$$S_2^s = -\frac{1}{4\pi}\int_0^\infty \frac{e^{-jkY}}{Y}\,\Lambda(\theta,x)\,dx \qquad (2.3.26)$$

The saddle point is again at $x = 0$ in which vicinity $\Lambda(\theta,x)$ is given by (2.3.14) and the integral is evaluated as previously demonstrated. Thus,

$$S_2^s \sim -\frac{2\cos\frac{\theta}{2}}{\pi}\,\frac{e^{-jk\bar{R}}}{\bar{R}}\int_0^\infty \frac{e^{-jkrr_0x^2/2\bar{R}}}{x^2 + (2\cos\frac{\theta}{2})^2}\,dx$$

$$\sim \mp\frac{e^{-jk\bar{R}}}{\sqrt{\pi\Delta_1\bar{R}}}\,e^{j\psi^2+j\frac{\pi}{4}}\,F(\psi)\ ,\ \text{for}\ \theta \lesssim \pi \qquad (2.3.27)$$

where $\psi = \left|\cos\frac{\theta}{2}\right|\ (2k\frac{rr_0}{\Delta_1\bar{R}})^{\frac{1}{2}}$, $\Delta_1 = 1 + 2\,\frac{rr_0}{\bar{R}^2}\cos^2\frac{\theta}{2}$ and the definitions (2.3.9) and (2.3.10) are used. This result agrees with Nomura's expression [60, equation 10] if Δ_1 is taken as unity.

2.4 Numerical Results

In order to test the accuracy of our approximate expressions, a comparison is made with available exact and other approximate solutions for a few numerical cases. In the evaluation of the solution for plane and cylindrical wave incidence, the asymptotic expressions (2.3.5) of the diffraction integrals, for the plane wave case, and (2.3.21) for cylindrical wave excitation, are used in addition to the geometrical optics terms.

Table 1 shows a comparison between our approximate expressions and the leading two terms in Pauli's expansion [43] for an H-polarized plane wave incident along the surface of a wedge with an exterior angle of 200°. The observation point in this case is along the shadow boundary. The results based on our expression are in better agreement with the exact values [71] than those based on Pauli's expansion. The accuracy of our asymptotic expression improves with increasing values of kr, as expected.

As another example, the exterior wedge angle is 190°, the angle of incidence is 0° and the field is calculated along the shadow boundary at $\phi = 180°$. Comparisons between the results based on our theory and those based on Pauli's [43], Hutchins [86] and Oberhettinger's [77] are presented in Figs. 2.2-2.4. These comparisons indicate that our results are in better agreement with the exact solution, as may be seen from Table 2, than those of Pauli's

Table 1

$\alpha = 200^\circ$, $\phi_0 = 0^\circ$, $\phi = 180^\circ$

H_z

kr	Exact Amplitude	Present Expression	Pauli's Theory
1	0.80747	0.81569	1.09957
2	0.76253	0.76598	0.85412
3	0.73234	0.73405	0.75477
4	0.70999	0.71088	0.69983
5	0.69255	0.69299	0.66469
6	0.67844	0.67862	0.64019
7	0.66674	0.66676	0.62210
8	0.65685	0.65676	0.60818
9	0.64835	0.64820	0.59713
10	0.64096	0.64076	0.58814

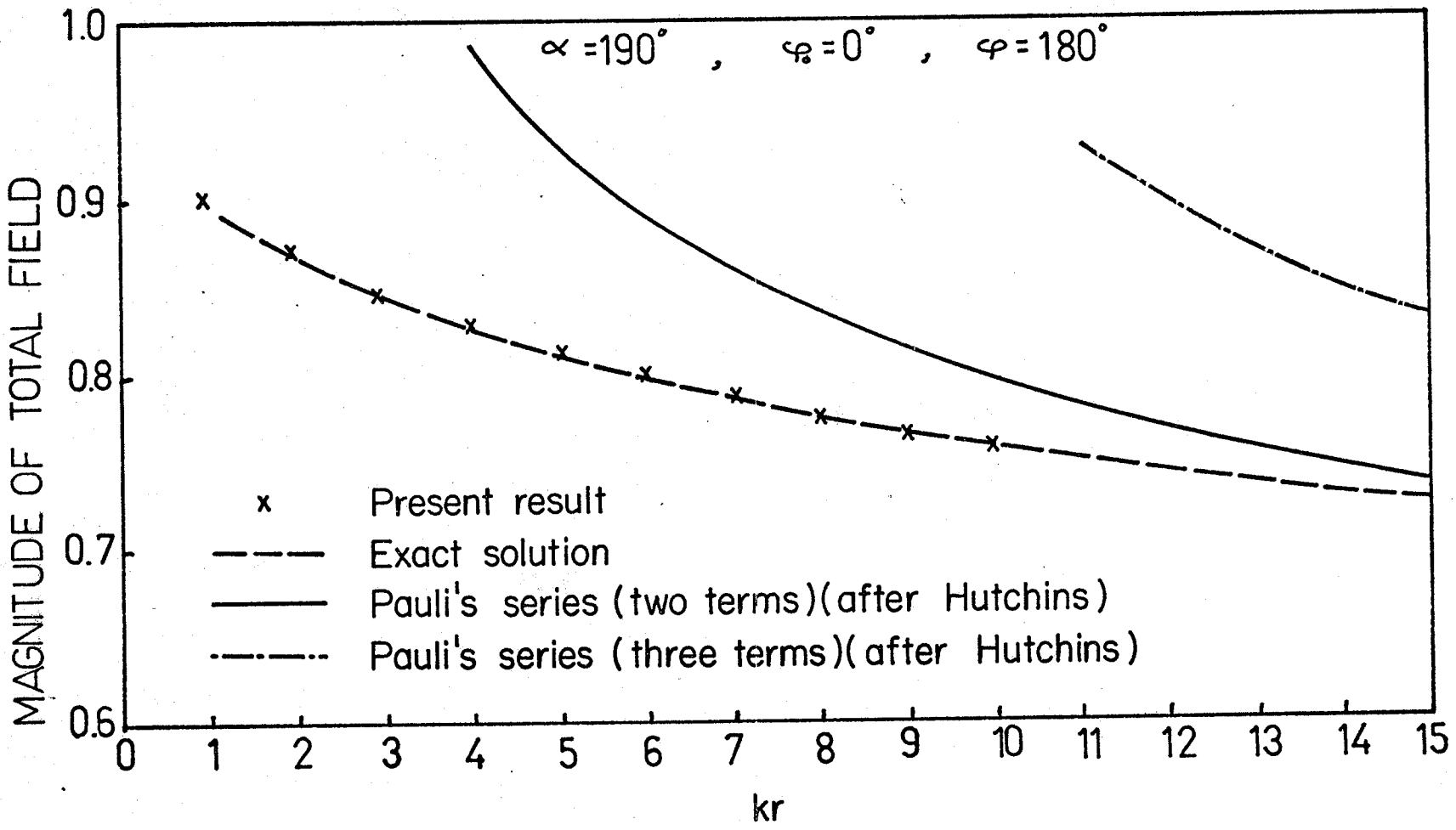

Fig. 2.2. Magnitude of the total field vs. kr for an H-polarized plane wave diffracted by a wedge (comparison between Pauli's series and the exact solution).

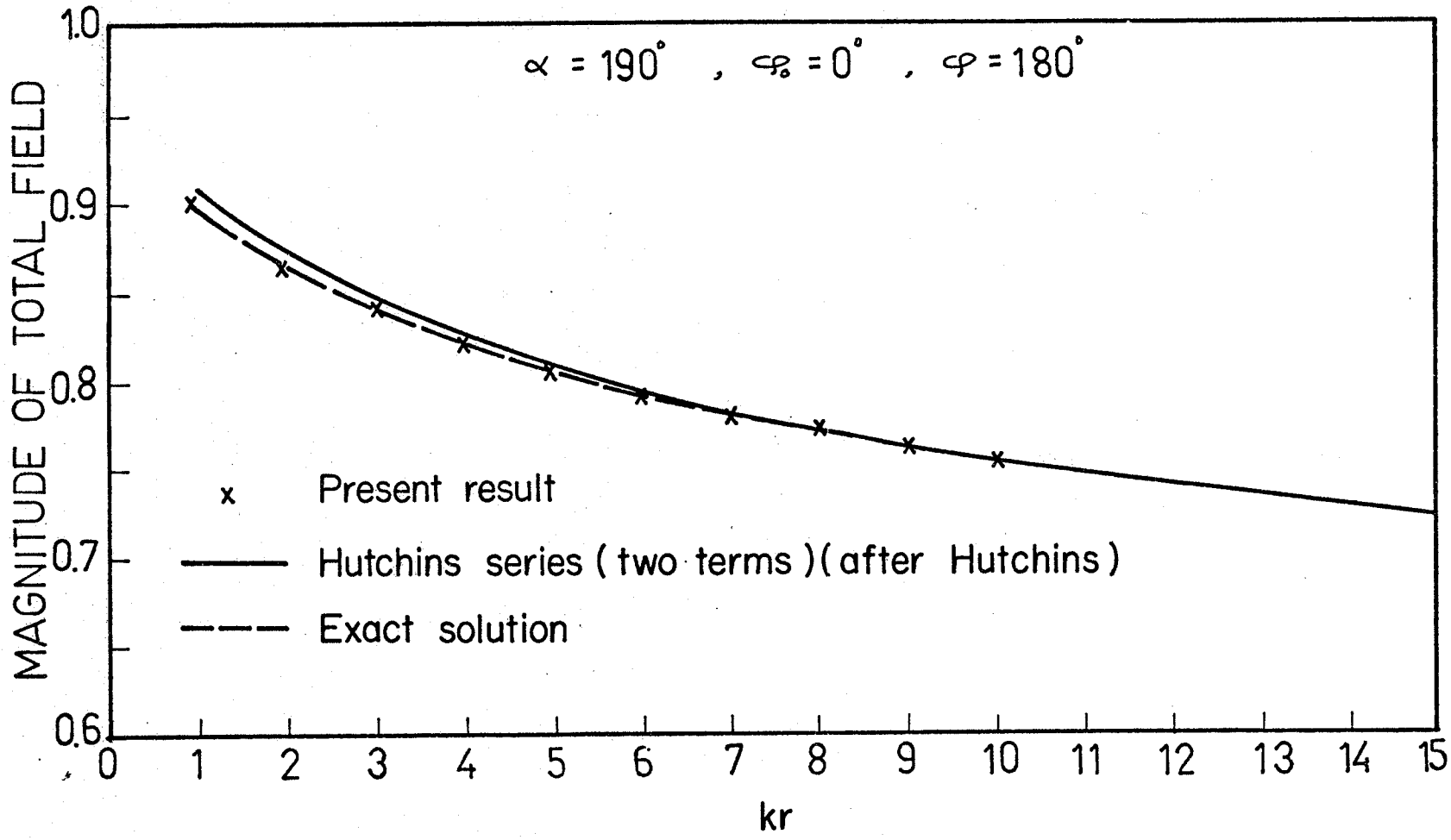

Fig. 2.3. Magnitude of the total field vs. kr for an H-polarized plane wave diffracted by a wedge (comparison between Hutchins' series and the exact solution).

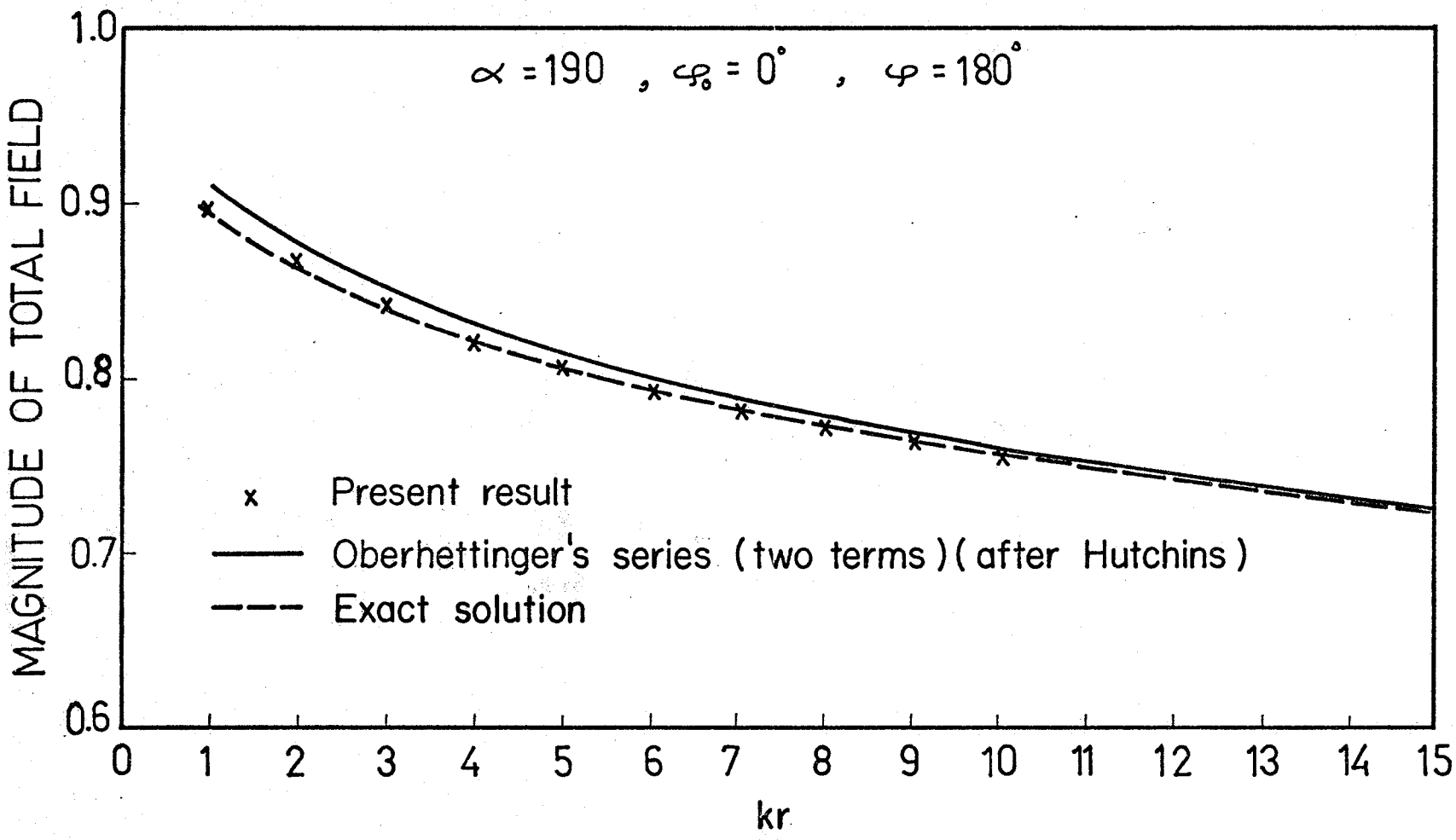

Fig. 2.4. Magnitude of the total field vs. kr for an H-polarized plane wave diffracted by a wedge (comparison between Oberhettinger's series and the exact solution).

Table 2

$\alpha = 190^\circ, \phi_0 = 0^\circ, \phi = 180^\circ$

H_z

kr	Amplitude		Phase (radians)	
	Exact	Approximate	Exact	Approximate
1	0.8950	0.9024	-1.0699	-1.0785
2	0.8647	0.8688	1.0470	1.0404
3	0.8422	0.8449	3.1583	0.9262
4	0.8239	0.8259	-0.9792	-0.9834
5	0.8086	0.8101	1.1543	1.1502
6	0.7954	0.7966	0.1481	0.1444
7	0.7838	0.7847	-0.8569	-0.8602
8	0.7734	0.7741	1.2808	1.2778
9	0.7640	0.7647	0.2776	0.2748
10	0.7556	0.7560	-0.7250	-0.7257

and Oberhettinger and compare favorably with Hutchins.

Table 3 shows a comparison between our approximate expression and the exact solution [71] for an H-polarized plane wave incident on a wedge, where $\alpha = 160^\circ$, $\phi_0 = 0^\circ$, $\phi = 160^\circ$, and kr varies from 0.1 to 10. This case represents a severe test on our formulation since the wedge angle is not only less than π but also kr is less than unity and the accuracy indicated gives more confidence in our theory.

For an H-polarized incident cylindrical wave, Table 4 presents a comparison between our approximate expression and the exact solution, which was computed using the series form, for a wedge with $\alpha = 200^\circ$, $\phi_0 = 20^\circ$, kr = 1, $\phi = 10^\circ$ and kr varies from 1 to 10. The comparison indicates that the present result is in good agreement with the exact value.

Table 3

$\alpha = 160^\circ$, $\phi_0 = 0^\circ$, $\phi = 160^\circ$

H_z

kr	Amplitude		Phase (radians)	
	Exact	Approximate	Exact	Approximate
0.1	1.109	1.130	0.064	0.044
0.2	1.089	1.097	0.141	0.122
0.3	1.067	1.067	0.226	0.209
0.4	1.045	1.040	0.316	0.302
0.5	1.022	1.015	0.411	0.401
0.6	1.001	0.993	0.512	0.504
0.7	0.982	0.973	0.616	0.612
0.8	0.965	0.956	0.725	0.723
0.9	0.951	0.943	0.836	0.837
1.0	0.940	0.934	0.951	0.953
5.0	0.989	0.990	-1.245	-1.245
10.0	0.991	0.991	0.548	0.548

Table 4

$\alpha = 200^\circ$, $\phi = 10^\circ$, $\phi_0 = 20^\circ$, $kr_0 = 1$

H_z

kr	Amplitude		Phase (radians)	
	Exact	Approximate	Exact	Approximate
1	2.664	2.607	0.763	0.726
2	1.490	1.536	-0.228	-0.213
3	1.118	1.155	-1.237	-1.223
4	0.930	0.962	0.899	0.915
5	0.812	0.841	-0.104	-0.087
6	0.730	0.756	-1.107	-1.089
7	0.668	0.692	1.033	1.051
8	0.620	0.642	0.032	0.050
9	0.581	0.602	-0.968	-0.950
10	0.541	0.568	1.172	1.191

CHAPTER 3

DIFFRACTION BY A CONDUCTING WEDGE LOADED BY A UNIFORM DIELECTRIC SLAB

3.1 Introduction

In Chapter 1 the importance of asymptotic wedge diffraction theory in the ray optical solutions of antenna problems was pointed out. In particular, the corner reflector antenna has multiple edges and the application of wedge ray diffraction is relevant for the analysis of such an antenna. This has been successfully demonstrated by Ohba [96] by taking into account the image as well as the edge diffracted rays. Corner reflector antennas are used as convenient sources of directive radiation in the UHF region. These antennas possess several desirable features such as high gain, low back radiation and wide bandwidth. Besides, their construction is simple and they can be readily built to fold into compact portable units. The dimensions are not critical since there are no focal points, as in the case of parabolic reflectors.

Several investigations have been carried out in order to modify the radiation characteristics of corner reflector antennas. Such modifications can be achieved by altering the type of feed as well as the shape of the wall and by

dielectric loading. The use of dielectric lenses in optical and microwave instrumentation is well known [97]. Depending on the location, shape and electrical characteristics of the dielectric, the radiation features of corner reflector antennas can be greatly modified. In particular, the effect of dielectric loading of the walls on the beamwidth and side lobes was experimentally verified by Hamid and Mohsen [98].

Examination of previous attempts to analyse the behavior of long corner reflector antennas indicates that the geometrical theory of diffraction is most promising for reasonable accuracy and physical understanding. However, this theory cannot be applied directly to deal with dielectric-loaded corner reflectors unless solutions are obtained to related canonical problems as discussed later. The asymptotic solutions of these problems may extend the applicability of the theory to dielectric-loaded corner reflectors as well as other diffracting bodies having similar configurations.

The main purpose of this chapter is, therefore, to deal with the asymptotic solution of an associated canonical problem, i.e. diffraction by a dielectric-loaded wedge.

In Chapter 2 we have dealt with the ray diffraction of plane, cylindrical and spherical waves by a conducting wedge. While the results proved to be in good agreement with exact solutions, the method is not directly applicable when one wall of the wedge is loaded by a dielectric slab. The

slab is of uniform thickness, which is assumed small relative to the wavelength, and of low relative dielectric constant (i.e. not much larger than unity).

In the first part of this chapter, an approximate solution for the problem of diffraction of plane waves by a perfectly conducting wedge, whose illuminated side is loaded by the dielectric slab, is derived. The scattered field is represented in an integral form and its value at the outer dielectric surface is assumed to be equal to the geometrical optics reflected field. After application of the boundary condition at the conducting surface and the use of an integral identity, the solution is written as the sum of geometrical optics terms and associated diffraction integrals. By comparison with the results of Chapter 2 for the unloaded wedge, the present solution is modified to take into account, in an approximate sense, the effect of edge diffraction at the dielectric surface. The diffraction integrals are of the same type considered in Chapter 2 and are evaluated in terms of Fresnel's integral.

In the second part, the results are extended to the cylindrical wave excitation by using the reciprocity principle to evaluate the far field. In this case, the geometrical optics terms are in agreement with those derived by Tai [99] for the dielectric-loaded plane. By comparison with the results of Chapter 2 an alternative expression which may be valid for smaller kr (provided $kr \gg kr_0$) is given.

3.2 Formulation for Plane Wave Incidence

3.2.1 *E-polarization*

Consider a plane electromagnetic wave incident on a perfectly conducting wedge of exterior angle α and which has the illuminated side loaded by a dielectric slab of relative permittivity ε_r and constant thickness τ, as shown in Fig. 3.1. The incident electric field is assumed parallel to the edge (i.e. E-polarization) and is given by

$$E_i = e^{jkr\cos(\phi-\phi_0)} \tag{3.2.1}$$

Following the procedure of Oberhettinger [66] the field of a cylindrical wave due to a line source at (r_0,ϕ_0) is expressed in terms of MacDonald's function as

$$H_0^{(2)}(kR_0) = \frac{4j}{\pi^2}\int_0^\infty K_{j\mu}(\gamma r)K_{j\mu}(\gamma r_0)\cosh[\mu(\pi-|\phi-\phi_0|)]d\mu \tag{3.2.2}$$

where $R_0 = [r^2+r_0^2-2rr_0\cos(\phi-\phi_0)]^{\frac{1}{2}}$ and $\gamma = jk$. The corresponding integral representation for plane waves may be obtained from (3.2.2) by employing the asymptotic forms of the Hankel and MacDonald's functions [89, p. 364 and p. 378] as $kr_0 \to \infty$, that is

$$H_0^{(2)}(kR_0) \sim (\frac{2}{\pi kr_0})^{\frac{1}{2}} e^{-jkr_0+j\frac{\pi}{4}} e^{jkr\cos(\phi-\phi_0)} \tag{3.2.3a}$$

and

$$K_{j\mu}(\gamma r_0) \sim (\frac{\pi}{2\gamma r_0})^{\frac{1}{2}} e^{-\gamma r_0} \tag{3.2.3b}$$

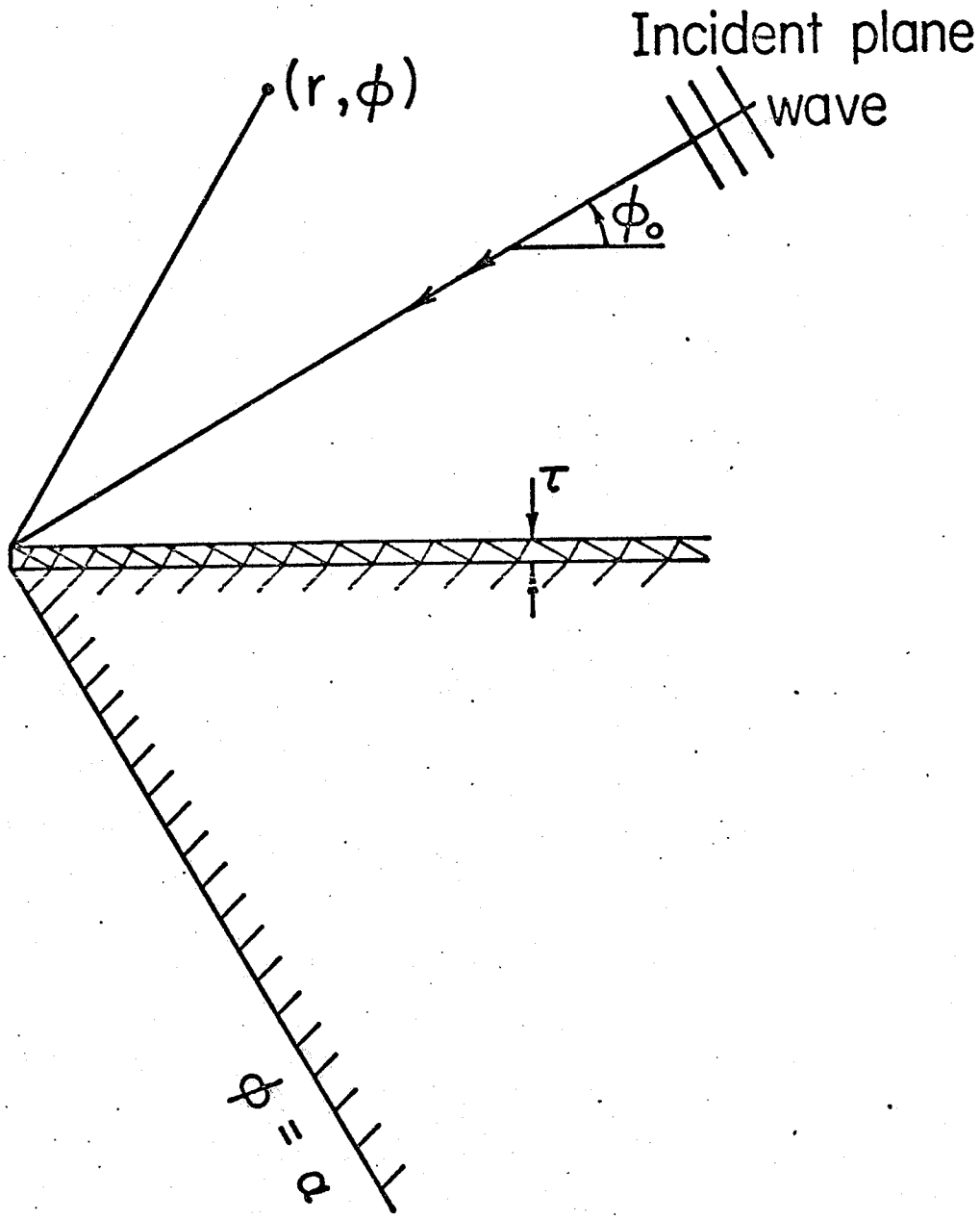

Fig. 3.1. Schematic diagram of a plane wave incident on a dielectric-loaded conducting wedge.

This leads to the expression

$$E_i = \frac{2}{\pi} \int_0^\infty K_{j\mu}(\gamma r)\cosh[\mu(\pi-|\phi-\phi_0|)]d\mu \qquad (3.2.4)$$

The scattered field due to plane wave incidence is assumed to have the representation

$$E_s = \frac{2}{\pi} \int_0^\infty K_{j\mu}(\gamma r)\{f_1(\mu)\cosh \mu\phi + f_2(\mu)\sinh \mu\phi\}d\mu \qquad (3.2.5)$$

which is an integral of fundamental solutions of the two-dimensional wave equation. The unknown function $f_1(\mu)$ and $f_2(\mu)$ are to be determined from the boundary conditions.

It should be noted that serious mathematical difficulties stand in the way of a rigorous solution of this problem since the configuration does not fit a separable coordinate system. At present, these difficulties make the accurate evaluation of the field in the slab and the application of the proper boundary conditions not possible. An approximate solution, however, is frequently sufficient for many practical applications of the loaded wedge, as discussed later. The first development of the approximate solution, presented next, neglects the contribution of the dielectric slab to the diffracted field at the dielectric surface. Obviously, the error introduced by this approximation becomes smaller as $\varepsilon_r \to 1$ and $k\tau \to 0$. Under these assumptions, the relation between the incident and scattered fields at $\phi = 0$ is assumed to be the same as in the case of a dielectric loaded plane. Thus, the boundary condition at $\phi = 0$ is taken

to be

$$E_s \simeq \Gamma_e E_i \tag{3.2.6}$$

where Γ_e is the well known parallel polarization reflection coefficient for a perfectly conducting plane loaded with a dielectric whose constitutive parameters are identical to those of the dielectric loading considered [94, p. 61]. Thus, Γ_e is given by

$$\Gamma_e = \Gamma_e(\theta_0) = \frac{r_e' - e^{-2j\delta'}}{1 - r_e' e^{-2j\delta'}}, \quad \theta_0 = \left|\frac{\pi}{2} - \phi_0\right| \tag{3.2.7}$$

where $\delta' = k\tau(\varepsilon_r - \sin^2\theta_0)^{\frac{1}{2}}$ and $r_e' = \dfrac{\cos\theta_0 - (\varepsilon_r - \sin^2\theta_0)^{\frac{1}{2}}}{\cos\theta_0 + (\varepsilon_r - \sin^2\theta_0)^{\frac{1}{2}}}$.

It should be noted that similar boundary conditions were successfully applied to solve for the diffraction of plane waves by a semi-infinite dielectric slab [100,101]. For the case of a perfectly conducting surface, it is obvious that as $\varepsilon_r \to \infty$ the value of Γ_e given by (3.2.7) equals -1 and, in this case, (3.2.6) gives the exact boundary condition.

Applying (3.2.6) to (3.2.4) and (3.2.5) we obtain

$$\int_0^\infty K_{j\mu}(\gamma r) f_1(\mu)\, d\mu = \Gamma_e \int_0^\infty K_{j\mu}(\gamma r) \cosh[\mu(\pi - \phi_0)]\, d\mu \tag{3.2.8a}$$

or

$$\int_0^\infty K_{j\mu}(\gamma r)\{f_1(\mu) - \Gamma_e \cosh[\mu(\pi - \phi_0)]\}\, d\mu = 0 \tag{3.2.8b}$$

The integral (3.2.8b) is in the form of a Lebedev transform

[102]. The inverse transform gives

$$f_1(\mu) \simeq \Gamma_e \cosh[\mu(\pi-\phi_0)] \tag{3.2.9}$$

Also, since the tangential electric field vanishes at a conducting surface, we have

$$E_i + E_s = 0 \qquad \text{at} \quad \phi = \alpha \tag{3.2.10}$$

This leads, in a manner similar to (3.2.9), to

$$\cosh[\mu(\pi-|\alpha-\phi_0|)] + f_1(\mu)\cosh \mu\alpha + f_2(\mu)\sinh \mu\alpha = 0 \tag{3.2.11}$$

Solving for $f_2(\mu)$ from (3.2.9) and (3.2.11), the total field takes the form

$$E^p = \frac{2}{\pi} \int_0^\infty K_{j\mu}(\gamma r) F(\mu) d\mu \tag{3.2.12}$$

where

$$F(\mu) = \cosh[\mu(\pi-|\phi-\phi_0|)] - \frac{\sinh \mu\phi}{\sinh \mu\alpha} \cosh[\mu(\alpha-\pi-\phi_0)]$$

$$+ \frac{\Gamma_e}{\sinh \mu\alpha} \cosh[\mu(\pi-\phi_0)] \sinh[\mu(\alpha-\phi)] \tag{3.2.13}$$

which completes the approximate integral solution of the problem. It is apparent from (3.2.12) and (3.2.13) that the solution consists of two parts one of which is independent of Γ_e, while the other is proportional to Γ_e. This indicates that the solution can be written as incident and reflected fields in addition to an associated diffracted field. Besides,

the integrals in (3.2.12) need to be evaluated, and this is performed next.

In order to evaluate the far field, the following integral is used

$$\int_0^\infty K_{j\mu}(\gamma r)\frac{\sinh \mu\beta}{\sinh \mu\alpha}\, d\mu = \frac{\pi}{2\alpha}\sin\frac{\pi\beta}{\alpha}\int_0^\infty \frac{e^{-\gamma r\cosh x}}{\cosh(\frac{\pi x}{\alpha})+\cos(\frac{\pi\beta}{\alpha})}\, dx\ ,$$

$$-\alpha<\beta<\alpha \qquad (3.2.14)$$

as shown in Appendix B. Also to fulfill the condition $-\alpha<\beta<\alpha$, we subdivide the region $0\le\phi\le\alpha$ of the exterior space. Thus, assuming α to be greater than $\pi+\phi_0$ and using the equalities

$$2\sinh \mu\phi \cosh \mu(\alpha-\pi-\phi_0) = \sinh \mu(\alpha-\pi+\phi-\phi_0)-\sinh \mu(\alpha-\pi-\phi-\phi_0)$$
$$2\sinh \mu\alpha \cosh \mu(\pi-|\phi\pm\phi_0|) = \sinh \mu(\alpha+\pi-|\phi\pm\phi_0|)+\sinh \mu(\alpha-\pi+|\phi\pm\phi_0|)$$
$$2\sinh \mu(\alpha-\phi)\cosh \mu(\pi-\phi_0) = \sinh \mu(\alpha+\pi-\phi-\phi_0)+\sinh \mu(\alpha-\pi-\phi+\phi_0)$$

and writing E^p as a sum of two terms, the second of which is dependent on Γ_e , that is

$$E^p = E_1^p + E_2^p \qquad (3.2.15)$$

we obtain

$$E_1^p = \frac{2}{\pi}\int_0^\infty K_{j\mu}(\gamma r)\left[\cosh \mu(\pi-|\phi-\phi_0|)-\frac{\sinh \mu\phi}{\sinh \mu\alpha}\cosh \mu(\alpha-\pi-\phi_0)\right]d\mu$$

$$= \begin{cases} e^{jkr\cos(\phi-\phi_0)}+\{I^p[\pi-(\phi-\phi_0),kr]-I^p[\pi+(\phi+\phi_0),kr]\}, & 0<\phi<\pi+\phi_0 \\ I^p[\pi-(\phi-\phi_0),kr]-I^p[\pi+(\phi+\phi_0),kr], & \pi+\phi_0<\phi<\alpha \end{cases} \qquad (3.2.16)$$

$$E_2^p = \frac{2}{\pi}\int_0^\infty K_{j\mu}(\gamma r)\,\frac{\sinh\mu(\alpha-\phi)\cosh\mu(\pi-\phi_0)}{\sinh\mu\alpha}\,\Gamma_e(|\tfrac{\pi}{2}-\phi_0|)$$

$$= \begin{cases} \Gamma_e(|\tfrac{\pi}{2}-\phi_0|)e^{jkr\cos(\phi+\phi_0)} + \Gamma_e(|\tfrac{\pi}{2}-\phi_0|)\{I^p[\pi-(\phi+\phi_0),kr] \\ \qquad - I^p[\pi+(\phi-\phi_0),kr]\}, \quad 0<\phi<\pi-\phi_0 \end{cases} \tag{3.2.17}$$

$$\begin{cases} \Gamma_e(|\tfrac{\pi}{2}-\phi_0|)\{I^p[\pi-(\phi+\phi_0),kr] - I^p[\pi+(\phi-\phi_0),kr]\}, \quad \pi-\phi_0<\phi<\alpha \end{cases} \tag{3.2.18}$$

where the integral $I^p(\delta,kr)$ is given by (2.3.2) and is evaluated asymptotically in section 2.3 for large values of kr, and the validity of the asymptotic evaluation is established by comparison with the exact solution in section 2.4. Comparing the diffraction integrals in (3.2.16) and (3.2.17) with those obtained in the solution for the perfectly conducting case, i.e. (2.3.1), it is found that the latter can be recovered if $(\phi\mp\phi_0)$, appearing in (3.2.16) and (3.2.17) is replaced by $|\phi\mp\phi_0|$. Thus, the new formulae which result for E_1^p and E_2^p are given by

$$E_1^p = \begin{cases} e^{jkr\cos(\phi-\phi_0)} + I_1(\phi,\phi_0,kr), \quad 0<\phi<\pi+\phi_0 & (3.2.19a) \\ I_1(\phi,\phi_0,kr), \quad \pi+\phi_0<\phi<\alpha & (3.2.19b) \end{cases}$$

and

$$E_2^p = \begin{cases} \Gamma_e(|\tfrac{\pi}{2}-\phi_0|)e^{jkr\cos(\phi+\phi_0)} + \Gamma_e(|\tfrac{\pi}{2}-\phi_0|)I_2(\phi,\phi_0,kr), \\ \qquad 0<\phi<\pi-\phi_0 & (3.2.20a) \\ \Gamma_e(|\tfrac{\pi}{2}-\phi_0|)I_2(\phi,\phi_0,kr), \quad \pi-\phi_0<\phi<\alpha & (3.2.20b) \end{cases}$$

where

$$I_1(\phi,\phi_0,kr) = I^p[\pi-|\phi-\phi_0|,kr] - I^p[\pi+|\phi+\phi_0|,kr] \qquad (3.2.21a)$$

$$I_2(\phi,\phi_0,kr) = I^p[\pi-|\phi+\phi_0|,kr] - I^p[\pi+|\phi-\phi_0|,kr] \qquad (3.2.21b)$$

Obviously, the boundary condition at $\phi=\alpha$ is still satisfied, while at $\phi = 0$ we have

$$E_1^p = e^{jkr\cos\phi_0} + \{I^p[\pi-|\phi_0|,kr] - I^p[\pi+|\phi_0|,kr]\}$$

and

$$E_2^p = \Gamma_e(|\tfrac{\pi}{2} - \phi_0|)\left\{e^{jkr\cos\phi_0} + \{I^p[\pi-|\phi_0|,kr] - I^p[\pi+|\phi_0|,kr]\}\right\}$$

i.e. the boundary condition (3.2.6) at $\phi=0$ is replaced by

$$E_2^p = \Gamma_e(|\tfrac{\pi}{2} - \phi_0|)E_1^p \qquad (3.2.22)$$

This condition, which relates the incident and reflected fields to the diffracted field at the dielectric surface, takes into account, in an approximate sense, the effect of edge diffraction at the dielectric surface.

Examination of (3.2.19) and (3.2.20) shows that the total field may be regarded as the sum of geometrical optics term and diffraction terms which are identified by the exponential and the $I^p(\delta,kr)$ terms, respectively. As in the case of a perfectly conducting wedge, each geometrical optics wave has an associated diffracted wave in all regions of the exterior space which are separated by shadow boundaries

at $\phi=\pi\pm\phi_0$. The continuity at the shadow boundaries requires the consideration of $\lim_{\delta\to 0} I^p(\delta,kr)$. As $\delta \to 0$ the integral $I^p(\delta,kr)$ vanishes except in the vicinity of $x = 0$ in which case

$$\frac{\sin\frac{\pi\delta}{\alpha}}{\cosh\frac{\pi x}{\alpha} - \cos\frac{\pi\delta}{\alpha}} \simeq \frac{\frac{\pi\delta}{\alpha}}{[1 + \tfrac{1}{2}(\frac{\pi x}{\alpha})^2] - [1 - \tfrac{1}{2}(\frac{\pi\delta}{\alpha})^2]} \simeq \frac{2\alpha}{\pi}\frac{\delta}{x^2+\delta^2} \qquad (3.2.23)$$

Since [103, p. 813]

$$\lim_{\delta\to\pm 0} \frac{\delta}{x^2+\delta^2} = (\pm)\ \pi\ \delta(x) \qquad (3.2.24)$$

we obtain

$$\lim_{\delta\to\pm 0} I^p(\delta,kr) = \pm\tfrac{1}{2}\int_{-\infty}^{\infty} e^{-jkr\cosh x}\ \delta(x)dx = \pm\frac{e^{-jkr}}{2} \qquad (3.2.25)$$

from which the continuity of E_1^p at $\phi=\pi+\phi_0$ and of E_2^p at $\phi=\pi-\phi_0$ follow.

It is interesting to note that although the field refracted in the dielectric and reflected at the wedge surface is not explicitly formulated, its approximate contribution is combined with the reflected field E_2^p. The resulting total field E^p has the same form as the solution for a perfectly conducting wedge presented in section 2.2 as expected. However, the amplitudes of the reflected wave and its associated diffracted field are proportional to Γ_e and hence are dependent on the thickness and relative

permittivity of the dielectric slab. This amplitude modification is required in calculating the geometrical optics and edge ray fields, as postulated in Keller's geometrical theory of diffraction.

3.2.2 *H-polarization*

For the case of an H-polarized incident plane wave, where the magnetic field H rather than the electric field E is parallel to the edge, we have for the incident magnetic field

$$H_i = e^{jkr\cos(\phi-\phi_0)} \tag{3.2.26}$$

Under the previous assumptions for the dielectric slab, (i.e. as in the case of E-polarization), the boundary condition at $\phi=0$ is taken as

$$\frac{\partial H_s}{\partial \phi} = \Gamma_h \frac{\partial H_i}{\partial \phi} \tag{3.2.27}$$

where H_s is the scattered magnetic field and Γ_h is the perpendicular polarization reflection coefficient for a dielectric loaded plane which is given by [94, p. 61]

$$\Gamma_h = \Gamma_h(\theta_0) = \frac{r_h - e^{-2j\delta'}}{1 - r_h e^{-2j\delta'}}, \quad \theta_0 = \left|\frac{\pi}{2} - \phi_0\right| \tag{3.2.28}$$

where

$$r_h = -\frac{\varepsilon_r \cos\theta_0 - (\varepsilon_r - \sin^2\theta_0)^{\frac{1}{2}}}{\varepsilon_r \cos\theta_0 + (\varepsilon_r - \sin^2\theta_0)^{\frac{1}{2}}}$$

For the case of a perfectly conducting surface, it is obvious that as $\varepsilon_r \to \infty$ the value of Γ_h equals -1 and, in this case, (3.2.26) gives the exact boundary condition. Using the integral representation (3.3.4) and (3.3.5) for H_i and H_s, respectively, and applying the boundary condition at the conducting surface, that is

$$\frac{\partial(H_s+H_i)}{\partial\phi} = 0 \ , \quad \text{at } \phi=\alpha \tag{3.2.29}$$

the total magnetic field takes the form

$$H^p = \frac{2}{\pi} \int_0^\infty K_{j\mu}(\gamma r)\ \bar{F}(\mu)\ d\mu \tag{3.2.30}$$

where

$$\bar{F}(\mu) = \cosh[\mu(\pi-|\phi-\phi_0|)] + \frac{\sinh\mu\phi}{\sinh\mu\alpha}\sinh[\mu(\pi-\alpha+\phi_0)] - \frac{\Gamma_h}{\sinh\mu\alpha}\sinh[\mu(\pi-\phi_0)]\cosh[\mu(\alpha-\phi)] \tag{3.2.31}$$

Employing the integral idnetity (3.2.14) and the subsequent approach for the E-polarization case, and comparing the resultant expression with that for the perfectly conducting case, the final expression for the total magnetic field may be written in the form $H^p = H_1^p + H_2^p$, where

$$H_1^p = \begin{cases} e^{jkr\cos(\phi-\phi_0)} + I_3(\phi,\phi_0,kr), & 0<\phi<\pi+\phi_0 \\ I_3(\phi,\phi_0,kr), & \pi+\phi_0<\phi<\alpha \end{cases} \tag{3.2.32}$$

and

$$H^p = -\begin{cases} \Gamma_h(|\frac{\pi}{2} - \phi_0|)e^{jkr\cos(\phi+\phi_0)} + \Gamma_h(|\frac{\pi}{2} - \phi_0|)I_4(\phi,\phi_0,kr) \\ \qquad 0<\phi<\pi-\phi_0 \\ \Gamma_h(|\frac{\pi}{2} - \phi_0|)I_4(\phi,\phi_0,kr), \quad \pi-\phi_0<\phi<\alpha \end{cases} \tag{3.2.33}$$

where

$$I_3(\phi,\phi_0,kr) = I^p[\pi+|\phi+\phi_0|,kr] + I^p[\pi-|\phi-\phi_0|,kr] \tag{3.2.34a}$$

$$I_4(\phi,\phi_0,kr) = I^p[\pi-|\phi+\phi_0|,kr] + I^p[\pi+|\phi-\phi_0|,kr] \tag{3.2.34b}$$

Similar to the E-polarization case, expressions (3.2.32) and (3.2.33) can each be identified as the sum of geometrical optics and diffraction terms.

3.3 Extension to Cylindrical Wave Incidence

The diffraction of a plane wave by a perfectly conducting wedge, whose illuminated side is loaded by a dielectric slab, has been discussed in the preceding section. However, the more general situation of cylindrical wave diffraction is of particular importance in the analysis of many types of antennas.

Because of the cylindrical nature of the incident field, plane wave diffraction cannot be directly applied to obtain the solution for cylindrical wave excitation. However, a solution may be obtained using the reciprocity principle by interchanging the observation and source points (this has been investigated in section 2.3.2).

Consider an E-polarized line source at (r_0,ϕ_0) and an observation point at (r,ϕ). The incident field $[H_0^{(2)}(kR_0)]$ is given in the far zone by [89, p. 364]

$$H_0^{(2)}(kR_0) \simeq \left(\frac{2}{\pi kR}\right)^{\frac{1}{2}} e^{-jkR_0+j\frac{\pi}{4}}$$

$$\sim \left(\frac{2}{\pi kr}\right)^{\frac{1}{2}} e^{-jkr+j\frac{\pi}{4}} \{e^{jkr_0\cos(\phi-\phi_0)}\} \qquad (3.3.1)$$

Using the reciprocity principle the far field due to line source excitation can be deduced from the plane wave case by replacing r and ϕ in the solution for the latter by r_0 and ϕ_0 and multiplying by $\left(\frac{2}{\pi kr}\right)^{\frac{1}{2}} e^{-jkr+j\frac{\pi}{4}}$. Thus for the case of a wedge angle $\alpha>\pi+\phi_0$, we write the total electric field as

$$E^c = E_1^c + E_2^c \tag{3.3.2}$$

where E_1^c and E_2^c may be written, using equations (3.2.19) and (3.2.20), in the form

$$E_1^c = \left(\frac{2}{\pi kr}\right)^{\frac{1}{2}} e^{-jkr+j\frac{\pi}{4}} \begin{cases} e^{jkr_0\cos(\phi-\phi_0)} + I_1(\phi,\phi_0,kr_0), & 0<\phi<\pi+\phi_0 \quad (3.3.3a) \\ I_1(\phi,\phi_0,kr_0), & \pi+\phi_0<\phi<\alpha \quad (3.3.3b) \end{cases}$$

$$E_2^c = \left(\frac{2}{\pi kr}\right)^{\frac{1}{2}} e^{-jkr+j\frac{\pi}{4}} \begin{cases} \Gamma_e(|\frac{\pi}{2}-\phi|)e^{jkr_0\cos(\phi+\phi_0)} \\ \quad + \Gamma_e(|\frac{\pi}{2}-\phi|)I_2(\phi,\phi_0,kr_0), & 0<\phi<\pi-\phi_0 \quad (3.3.4a) \\ \Gamma_e(|\frac{\pi}{2}-\phi_0|)I_2(\phi,\phi_0,kr_0), & \pi-\phi_0<\phi<\alpha \quad (3.3.4b) \end{cases}$$

It should be noted that although in the derivation of (3.2.19) and (3.2.20) the assumption that the plane wave illuminates the dielectric-loaded surface was employed, the field expressions (3.3.3b) and (3.3.4b) in the shadow regions are written such that continuity is ensured at the shadow boundaries and the field vanishes at the conducting surface.

It is interesting to note that the first terms of (3.3.3a) and (3.3.4a) are identical to the geometrical optics terms due to the incident and reflected waves, as also given by Tai [99] for a dielectric-loaded plane. The reflected wave corresponds to a wave due to the image of the source with respect to the dielectric surface modified by a plane

wave reflection coefficient corresponding to an angle of incidence equal to that between the normal to the dielectric surface and the line joining the image and the observation point.

In order to extend the validity of (3.3.3) and (3.3.4) to smaller values of kr (provided that $kr>>kr_0$), the following argument is used. On the basis of the analogy between the cylindrical and plane wave excitations, which has already been demonstrated for the unloaded wedge in Chapter 2, it is postulated that the diffraction integral $I^p(\delta,kr)$ employed in the plane wave formulation, for both the loaded and unloaded wedge, should be replaced by the corresponding integral $I^c(\delta,kr,kr_0)$, given by equation (2.3.18), for a cylindrical wave incident on an unloaded wedge. Thus for $kr>>kr_0$, the resulting formulas for E_1^c and E_2^c are given by

$$E_1^c = \begin{cases} H_0^{(2)}(kR_0) + \{I^c[\pi-|\phi-\phi_0|,kr,kr_0] - I^c[\pi+|\phi+\phi_0|,kr,kr_0]\}, \\ \qquad\qquad 0<\phi<\pi+\phi_0 \\ I^c[\pi-|\phi-\phi_0|,kr,kr_0] - I^c[\pi+|\phi+\phi_0|,kr,kr_0], \quad \pi+\phi_0<\phi<\alpha \end{cases} \tag{3.3.5}$$

and

$$E_2^c = \begin{cases} \Gamma_e(|\frac{\pi}{2}-\phi|)H_0^{(2)}(kR_1) + \Gamma_e(|\frac{\pi}{2}-\phi|)\{I^c[\pi-|\phi+\phi_0|,kr,kr_0] \\ \qquad - I^c[\pi+|\phi-\phi_0|,kr,kr_0]\}, \quad 0<\phi<\pi-\phi_0 \\ \Gamma_e(|\frac{\pi}{2}-\phi_0|)\{I^c[\pi-|\phi+\phi_0|,kr,kr_0] - I^c[\pi+|\phi-\phi_0|,kr,kr_0]\} \\ \qquad\qquad \pi-\phi_0<\phi<\alpha \end{cases} \tag{3.3.6}$$

where $R_1 = [r^2+r_0^2-2rr_0\cos(\phi+\phi_0)]^{\frac{1}{2}}$ is the distance from the observation point to the image. It may be shown that (3.3.5) and (3.3.6) reduce to (3.3.3) and (3.3.4), respectively, as $kr\to\infty$. This follows directly from the asymptotic expressions for the Hankel functions (3.3.1) and the diffraction integral $I^c(\delta,kr,kr_0)$ given by (2.3.21).

Although only the E-polarization is presented here, it should be noted that the H-polarization can be treated in a similar fashion by employing the reciprocity principle and using (3.2.31) and(3.2.32).

CHAPTER 4

APPLICATION TO A DIELECTRIC-LOADED STRIP

4.1 Introduction

As already pointed out the use of dielectrics for modifying the radiation characteristics of wedge-shaped antennas is both desirable and feasible. This is obviously subject to the electrical and geometrical parameters of the loading.

The main purpose of this chapter is to employ the ray optical solution derived in Chapter 3 for a dielectric-loaded wedge in order to study the effect of uniform dielectric loading of the walls of corner reflectors. The theory is applied to study the effect of dielectric loading on the H-plane radiation pattern of a strip, illuminated by an E-polarized dipole whose axis is parallel to the edges of the strip.*

The theoretical formulation of the radiation pattern is based on equations (3.3.3) and (3.3.4) and takes into account the geometrical optics terms as well as the diffraction terms due to the edges. The geometrical optics terms are due to the contributions of the source and the image

---

* It should be pointed out that the unloaded strip has been successfully analyzed by ray theory [104].

relative to the outer dielectric surface as indicated in section 3.3. The edge terms are due to the diffraction of the incident wave at both edges of the strip. Here each edge is treated as that of a dielectric-loaded half-plane. Besides the restrictions on the dielectric constant and the thickness of the slab, the electrical width of the strip is assumed to be sufficiently large so that the higher order edge-edge interaction terms can be neglected. By summing the contributions from the geometrical optics and singly diffracted rays passing through the observation point and plotting the far field as a function of angle, the radiation pattern is obtained. The results are found to be in good agreement with experiment for different conditions, showing that the approximations used in Chapter 3 are valid.

4.2 Formulation

Consider a perfectly conducting strip of width 2W fed by a dipole whose axis is parallel to the edges and situated at a distance s from the metallic surface as shown in Fig. 4.1. The strip is loaded by a uniform dielectric slab of thickness τ (which is small relative to the wavelength) and relative permittivity ε_r (which is assumed not much larger than unity).

A basic assumption in the calculations is that W is large relative to the wavelength so that the solution for the dielectric-loaded half-plane may be employed with A and B as diffracting edges. The theory developed in Chapter 3 for the diffraction of a cylindrical wave by a dielectric-loaded half-plane ($\alpha = 2\pi$) is also considered adequate in this case since only the H-plane ($\rho - \theta$) radiation pattern is of interest.

The total field at the observation point Q is the sum of a geometrical optics as well as an edge diffraction term due to A and B. Higher order edge-edge interaction terms are neglected since they are zero in the absence of the dielectric for the E-polarization and they are assumed small in the presence of the dielectric due to our assumptions on ε_r and τ. The geometrical optics term is due to the direct ray from the source [0] and a reflected ray viewed as emanating from the image source [1], which is the image of the primary source with respect to the dielectric surface

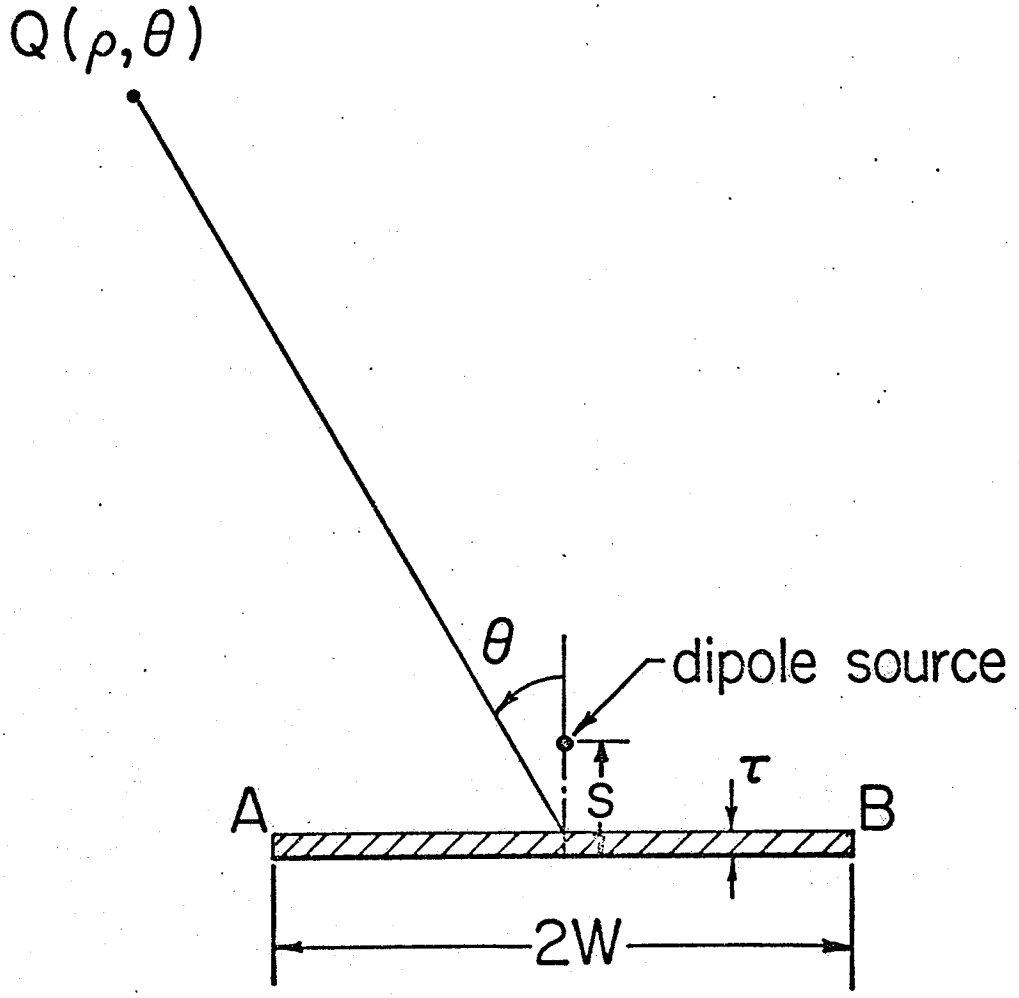

Fig. 4.1. Schematic diagram of a dielectric-loaded conducting strip fed by a dipole source.

AB, as discussed in section 3.3. Thus, using (3.3.3) and (3.3.4), the normalized geometrical optics contributions due to the primary and image sources denoted by I_0 and I_1, respectively, are given by

$$I_0 = e^{jk\bar{s}\cos\theta} \tag{4.2.1}$$

and

$$I_1 = \Gamma_e(\theta)\ e^{-jk\bar{s}\cos\theta} \tag{4.2.2}$$

where the normalization factor

$$\left(\frac{2}{\pi k\rho}\right)^{\frac{1}{2}}\ e^{-jk\rho+j\frac{\pi}{4}}$$

is employed, $\bar{s} = s - \tau$ and $\Gamma_e(\theta)$ is the reflection coefficient of the dielectric surface.

Based on the analysis outlined in section 3.3, the formularion of the z-component of the electric field in the H-plane depends on the location of the observation point within the various regions of diffraction. To identify these, the space outside the strip is subdivided by planes across which the incident or reflected ray appears or disappears. Another subdivision is made by the plane containing the two edges. Due to the symmetry of the problem, only values of θ between 0° and 180° are considered. Thus, for these values of θ, the total number of diffraction regions is four as shown in Fig. 4.2, where $0 \leq \theta < \theta_1 = \tan^{-1}\frac{W}{\bar{s}}$ in region I, $\theta_1 \leq \theta < \theta_2 = \frac{\pi}{2}$ in region II, $\theta_2 \leq \theta < \theta_3 = \pi - \theta_1$ in region

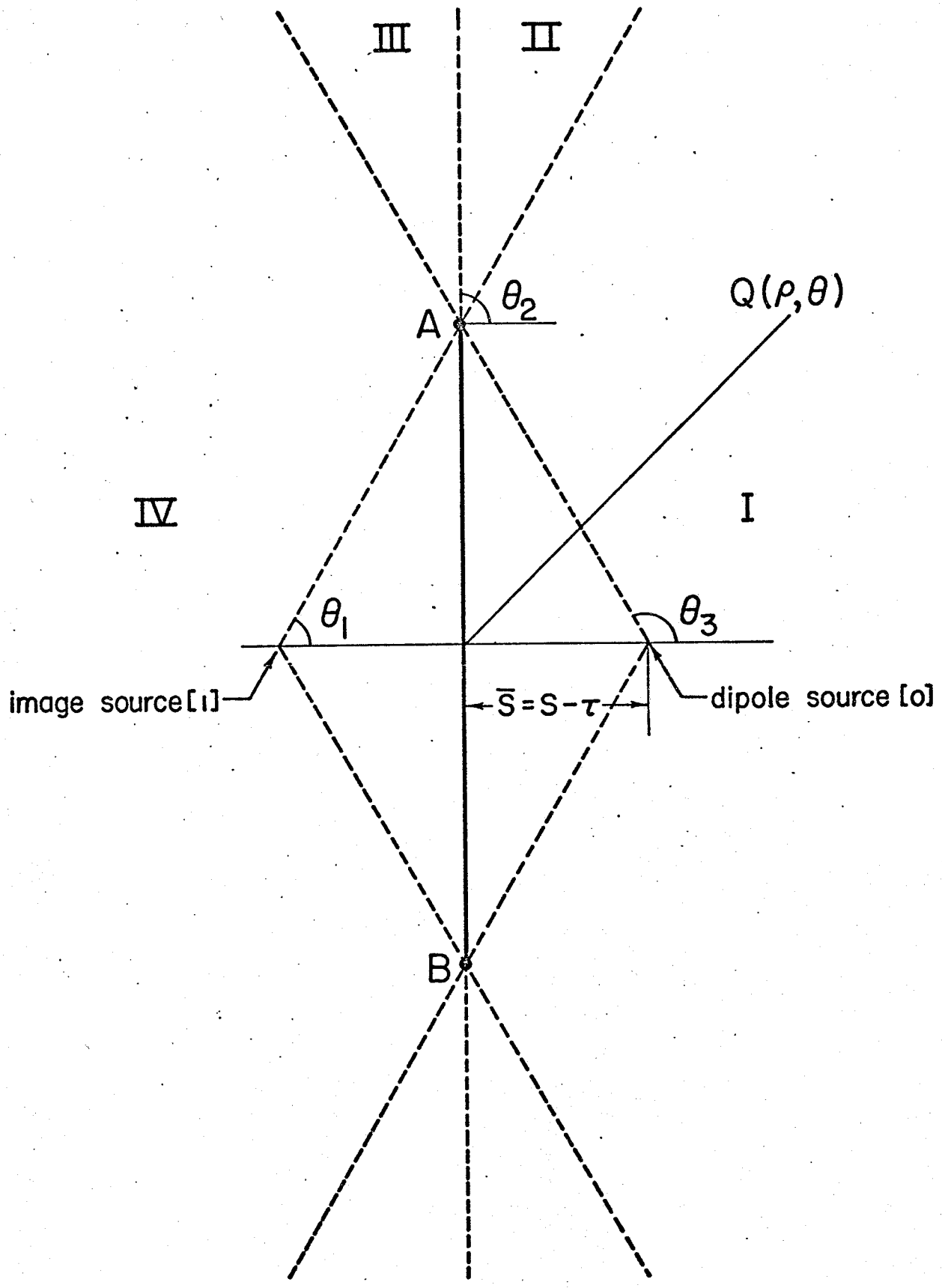

Fig. 4.2. Different regions of space for the strip geometry.

III, and $\theta_3 \leq \theta \leq \pi$ in region IV. Thus, the normalized far field due to a ray emanating at [0] and diffracted at A may be written, using (3.3.3) and (3.3.4), in the form

$$I(0,A) = e^{jkW\sin\theta}\, I_1(\tfrac{\pi}{2}+\theta,\phi_0,d) \tag{4.2.3}$$

where ϕ_0 is the angle of incidence measured with respect to AB (i.e. $\phi_0 = \tan^{-1}\frac{\bar{s}}{W}$) while d is the distance from [0] to A (i.e. $d^2 = \bar{s}^2 + W^2$). Similarly, the term due to the ray emanating from the image source [1] and diffracted at A is denoted by $I^{\mp}(1,A)$ and is given by

$$I^{\mp}(1,A) = e^{+jkW\sin\theta}\, I_2(\tfrac{\pi}{2}+\theta,\phi_0,d) \begin{cases} \Gamma_e(\theta) & 0\leq\theta<\theta_1 \\ \Gamma_e(\theta_1) & \theta_1\leq\theta<\pi \end{cases} \tag{4.2.4}$$

Similarly, the field of the rays diffracted at B due to [0] and [1] are given by

$$I^{\mp}(0,B) = e^{-jkW\sin\theta} \begin{cases} I_1(\tfrac{\pi}{2}-\theta,\phi_0,d) & 0\leq\theta<\theta_2 \\ I_1(\tfrac{5\pi}{2}-\theta,\phi_0,d) & \theta_2\leq\theta\leq\pi \end{cases} \tag{4.2.5}$$

and

$$I^{\mp}(1,B) = e^{-jkW\sin\theta} \begin{cases} \Gamma_e(\theta)\, I_2(\tfrac{\pi}{2}-\theta,\phi_0,d) & 0\leq\theta<\theta_2 \\ \Gamma_e(\theta_1)\, I_2(\tfrac{5\pi}{2}-\theta,\phi_0,d) & \theta_2\leq\theta\leq\pi \end{cases} \tag{4.2.6}$$

Thus, when the field point Q is in any of the four regions, the normalized z-component of the electric field in the H-plane is obtained by the sum of the contributions of all

the rays passing through it, and is given by

Region I:

$$E = I_0 + I(0,A) + I^-(0,B) + I_1 + I^-(1,A) + I^-(1,B) \qquad (4.2.7)$$

Region II:

$$E = I_0 + I(0,A) + I^-(0,B) + I^+(1,A) + I^-(1,B) \qquad (4.2.8)$$

Region III:

$$E = I_0 + I(0,A) + I^+(0,B) + I^+(1,A) + I^+(1,B) \qquad (4.2.9)$$

Region IV:

$$E = I(0,A) + I^+(0,B) + I^+(1,A) + I^+(1,B) \qquad (4.2.10)$$

It should be noted that the total electric field E is continuous everywhere, as shown in section 3.2.1, except for the plane of the strip ($\theta = 90^\circ$). However, the discontinuity of the field in this plane is numerically small due to our previous assumptions on τ and ε_r and may be reduced further if edge-edge interactions are considered.

4.3 Experimental Verification

The experimental set-up used to verify the theoretical results is shown schematically in Fig. 4.3. The experiment was carried out in a microwave anechoic chamber to simulate free space conditions. A transmitting 60° corner reflector antenna was fed by a half-wave dipole tuned to a frequency of 3 GHZ and modulated by a 1 KHZ signal. The reflector dimensions were chosen such that a suitable directivity for illuminating the test strip is achieved, and the side-lobes of its radiation pattern are sufficiently low in order to reduce the undesirable effects of the chamber walls. A copper sheet of dimensions 11" x 25" fed by a half-wave dipole was used as a receiver and situated in the far field of the transmitter. The height was taken long enough ($\simeq 6.35\lambda$) to reduce the contribution of the upper and lower edges of the sheet to the radiation pattern, particularly back radiation, and were therefore covered with absorbing material. Two adjustable stubs were employed for matching the receiving antenna to its own receiver. Absorbing material was also used to cover all other objects in the immediate vicinity which were thought to interfere with the experiment.

The experiment was first carried out for the unloaded strip with $s = 0.4\lambda$ and the comparison between experimental and theoretical results is shown in Fig. 4.4 where the field is normalized to the maximum.

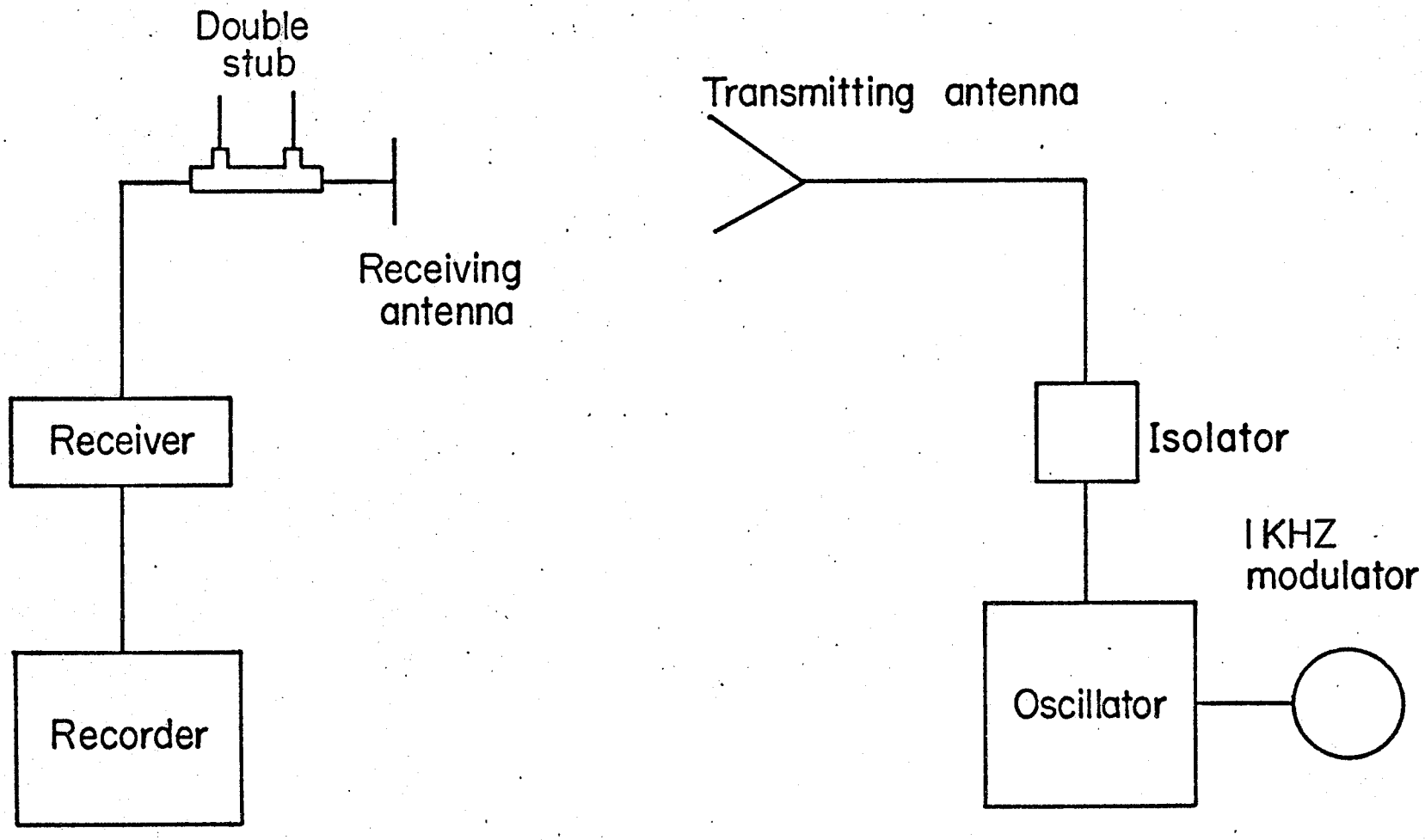

Fig. 4.3. Experimental set-up for measuring the radiation pattern of a dielectric-loaded strip.

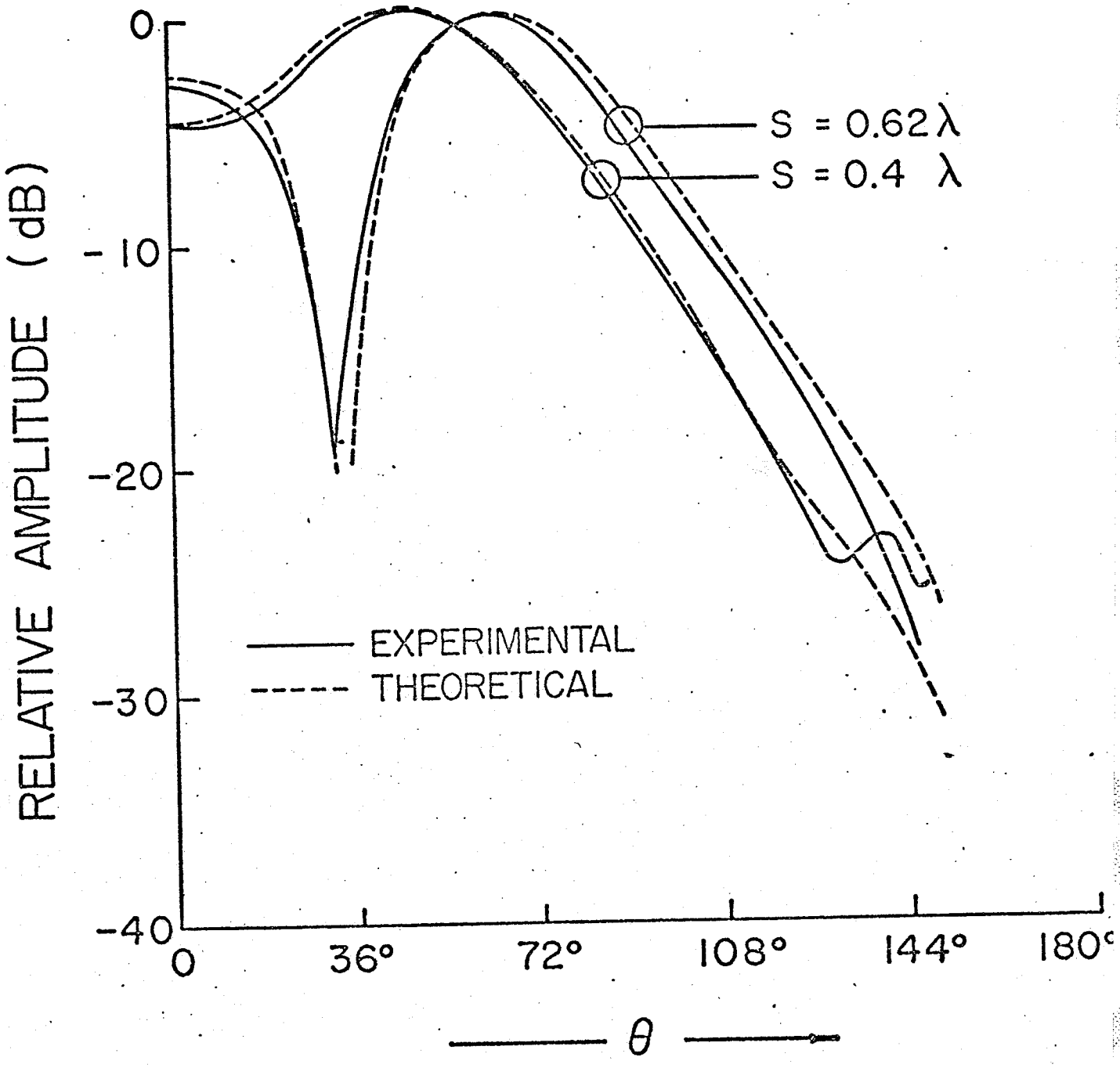

Fig. 4.4. Radiation pattern of the unloaded strip.

The measurements were repeated for a plexiglas-loaded strip with $\varepsilon_r = 2.59$, $\tau = 0.127\lambda$ and the comparison between theory and experiment is shown in Fig. 4.5.

A similar experiment was performed for $s = 0.62\lambda$ and $\tau = 0, 0.127\lambda$ and the experimental as well as theoretical results are given in Figs. 4.4 and 4.5.

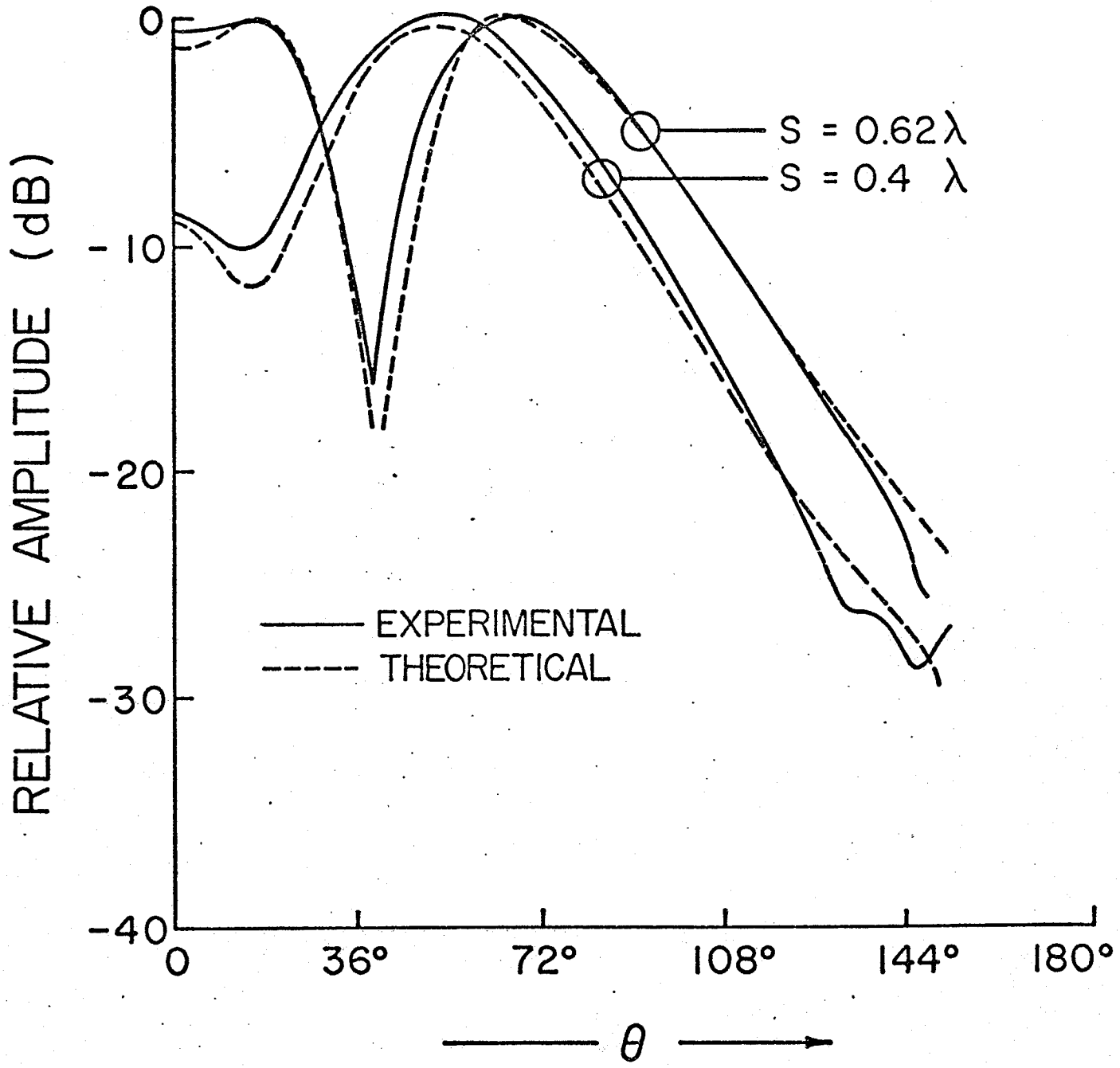

Fig. 4.5. Radiation pattern of the loaded strip ($\tau = 0.127\lambda$).

CHAPTER 5

DISCUSSION

Asymptotic diffraction of waves by a dielectric-loaded and unloaded wedge is treated in this thesis. In the latter problem, the diffraction of plane, cylindrical and spherical waves by a perfectly conducting wedge is considered (Chapter 2). The diffraction integrals encountered are evaluated, using the saddle point method, on the assumption that both observation and source points are far away from the edge (section 2.3). The main feature of the result is that all the asymptotic formulas are in terms of Fresnel's integral and are approximated to a sufficient degree of accuracy by only one term. The asymptotic evaluation of the diffraction terms for plane wave diffraction by a half-plane [equation (2.3.16)], using the same technique, yields the well known Sommerfeld's expression [43]. Expressions (2.3.21) for cylindrical and (2.3.24) for spherical wave incidence reduce to those of Lewin [46] and Whipple [95] respectively, for $r>>r_0$ and $kr_0>>1$ or $r<<r_0$ and $kr>>1$. This conclusion relates the results to known expressions which were derived by different approaches. Further confidence in the present result is established by favourable comparison with the exact solution and known asymptotic expressions.

The numerical results presented in section 2.4 are based on the asymptotic expressions (2.3.5) and (2.3.21) for the diffraction integrals, for H-polarized plane wave and cylindrical wave excitations, respectively, in addition to the geometrical optics terms. In Table 1, a comparison between our approximate result and that based on the first two terms in Pauli's asymptotic expansion [43] is presented for plane wave diffraction by a wedge with $\alpha = 200°$, $\phi_0 = 0°$, $\phi = 180°$. The exact solution indicates a decay in the amplitude of the field as the observation point is moved away from the edge. Our result is in close agreement with the exact solution even for kr as low as unity where the deviation is about 1.1%. The accuracy improves with increasing values of kr, as expected, and the error reduces to 0.03% at kr = 10. The result based on Pauli's expansion is not as accurate as the present result, since the deviation in the former result from the exact solution is about 36.2% for kr = 1 and reduces to 0.75% for kr = 10.

Figure 2.2 represents another comparison for the case $\alpha = 190°$, $\phi_0 = 0°$, $\phi = 180°$. The general behavior of the field is almost the same as for the previous example but the amplitude is higher. As concluded by Hutchins [86], Pauli's series fails to yield an accurate value for the field regardless of the number of terms used. The deviation using the series, for this particular case, increases if three terms are used instead of two. Again, our result is

in excellent agreement with the exact solution, for both amplitude and phase, in the entire range considered, kr = 1 to 10, as may be seen from Table 2. Figure 2.3 represents a comparison between our result and Hutchins' asymptotic expansion [86] up to the second term. The comparison indicates that both results are in good agreement with the exact solution but our result is more accurate. The reason for our improved accuracy, for the same number of terms, over Pauli's and Hutchins' expressions is due to the use of different integral representation for the solution of the problem. The comparison between our result and Oberhettinger's [67], using two terms in his expansion, is given in Fig. 2.4 and indicates that our result is in better agreement with the exact solution. The reason for our improved accuracy, in this case, is due to the application of the saddle point principle rather than Watson's lemma as applied by Oberhettinger.

For $\alpha<\pi$ both Pauli's and Oberhettinger's expansions are invalid [86]. In contrast, Table 3 shows a comparison between our result and the exact solution for $\alpha = 160°$, $\phi_0 = 0°$, $\phi = 160°$ and kr assumes values from 0.1 to 10. This comparison indicates that our result is in excellent agreement with the exact solution for both amplitude and phase. This case represents a severe test on our expansion for not only is the wedge angle less than π but also kr is less than unity and the accuracy indicated gives more

confidence in our theory.

Table 4 shows a comparison between our results and the exact solution for cylindrical wave excitation with $\alpha = 200°$, $\phi_0 = 20°$, $kr_0 = 1$, $\phi = 10°$ and kr varying from 1 to 10. The result indicates a decay in the amplitude of the field with increasing kr. This result is in good agreement with the exact solution for both amplitude and phase and the agreement improves with increasing kr. From (2.3.21) the deviation from the exact solution decreases with increasing kr_0 since in this case the error resulting from the asymptotic approximation decreases.

The effect of loading the illuminated side of the wedge is considered in Chapter 3 for plane and cylindrical wave excitation. The geometrical optics terms, for cylindrical wave incidence, are identical to those derived by Tai [99] for the case of a dielectric-loaded plane. Tai treated this case as a boundary value problem and evaluated the radiation field using the saddle point method. He concluded that the reflected wave represents the dominant scattered wave in the far field, away from the dielectric surface, even if the slab is thick enough to support a surface wave. If the thickness of the slab is larger than the critical thickness [99], (i.e. $\tau = \frac{\lambda}{4(\varepsilon_r - 1)^{\frac{1}{2}}}$), a surface wave appears in the neighborhood of the interface. Tai showed that this wave attenuates exponentially as the point of observation is moved away from this interface.

It is on this basis, as well as on the assumptions on τ and ε_r, that the surface wave contribution is neglected in the present work.

The diffraction integrals encountered are of the same type dealt with for the unloaded case. The diffraction terms associated with the reflected wave (equations (3.2.20) and (3.2.33)) are proportional to the reflection coefficient Γ_e (or Γ_h) for the E (or H) polarization.

Investigation of expression (3.2.7) for Γ_e indicates that this quantity remains unchanged when δ' is replaced by $\delta' \pm n\pi$ (n is integer), i.e. when τ is replaced by $\tau \pm \Delta\tau$ where

$$\Delta\tau = \frac{n\lambda}{2(\varepsilon_r - \sin^2\theta_0)^{\frac{1}{2}}}$$

Thus, the radiation field remains unchanged if the thickness of the slab is changed by $\Delta\tau$. Also, Γ_e equals (+1) if $\delta' = (2n+1)\frac{\pi}{2}$, i.e. if $\tau(\varepsilon_r - \sin^2\theta_0)^{\frac{1}{2}} = \frac{(2n+1)\lambda}{4}$, and equals (-1) when $\delta' = n\pi$, i.e. when $\tau(\varepsilon_r - \sin^2\theta_0)^{\frac{1}{2}} = \frac{n\lambda}{2}$. Such values of δ' can be realized by altering τ, ε_r or θ_0 or any combination of these parameters to achieve the required value. It should be noted that if $\Gamma_e = +1$ the problem will be identical to that of diffraction of an H-polarized wave by an unloaded conducting wedge while $\Gamma_e = -1$ corresponds to the case of diffraction of an E-polarized wave. Thus, the parameters of the dielectric loading can be chosen to control the radiation pattern to a great extent.

The effect of varying the dielectric constant on the radiation pattern of a line source in the presence of a grounded dielectric slab is demonstrated in Fig. 5.1. Only the geometrical optics terms, i.e. the first term in each of (3.3.3) and (3.3.4), are needed in the evaluation of the field. The distance s from the line source to the plane equals $\frac{\lambda}{2}$ and the radiation patterns in this figure are normalized to their respective maxima. For the unloaded case the pattern consists of two lobes whose maxima are at ±60° and the 3-dB beamwidth is about 37°. If the plane is covered by a dielectric of thickness $\tau = \frac{\lambda}{4}$ and $\varepsilon_r = \sqrt{2}$ the resulting pattern consists of three lobes whose maxima are at 0°, ±66° and the beamwidth of the main lobes (whose maxima are at ±66°) becomes 32°. If $\varepsilon_r = 2$ the pattern consists of only two lobes where the locations of the main lobes move close to the dielectric surface ($\theta = \pm 89°$) while the beamwidth of these lobes increases to 39°. If the relative dielectric constant ε_r is increased to 2.5 the radiation pattern will consist of only one lobe whose location is away from the dielectric surface (at $\theta = 0°$) and whose beamwidth is increased substantially to 76°. This indicates that dielectric loading has a significant effect on the radiation pattern in terms of the beamwidth as well as the number and location of lobes.

It is interesting to examine the relative effects of

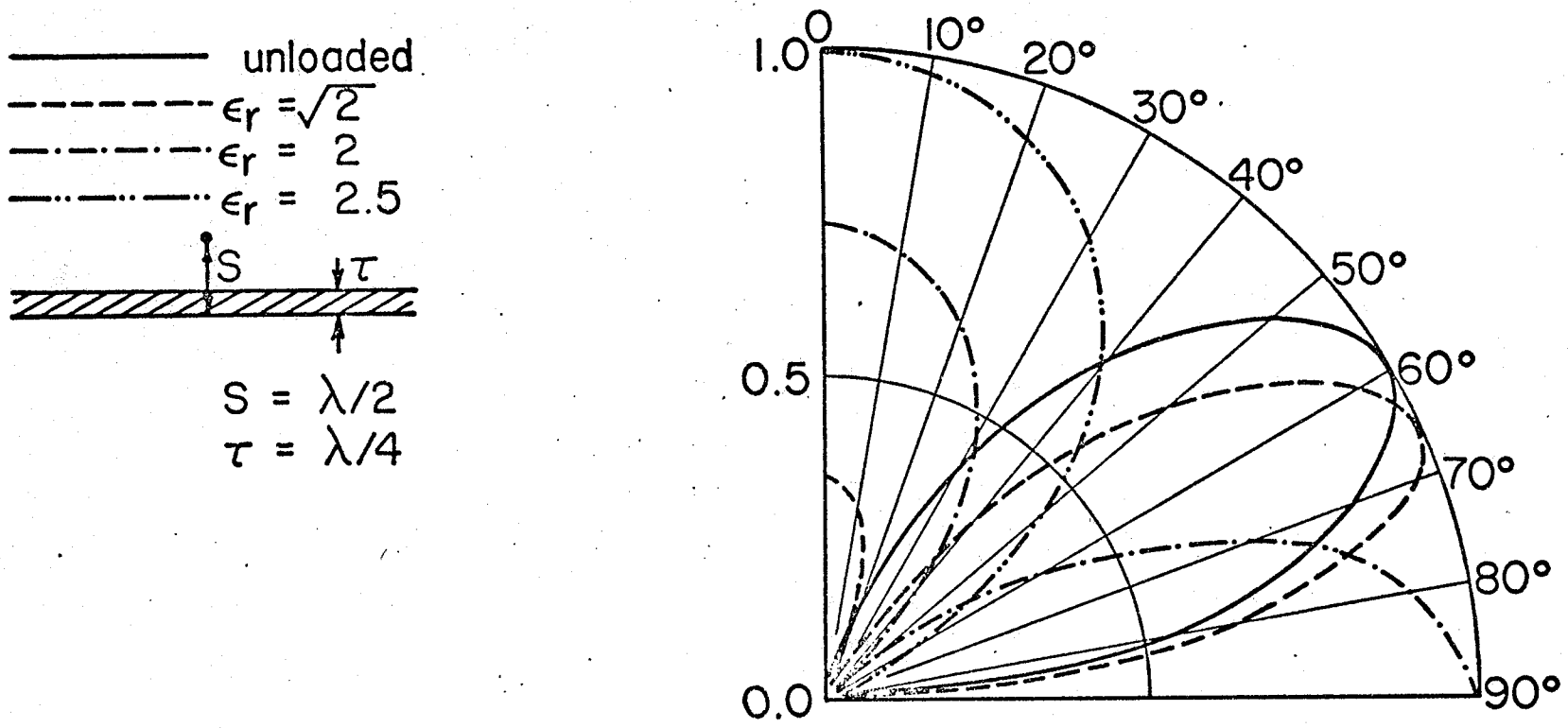

Fig. 5.1. Radiation pattern of a dielectric-loaded conducting plane.

geometrical and edge diffraction terms on the radiation pattern of the dielectric-loaded strip. Figure 5.2 shows the radiation pattern for an unloaded strip ($s = 0.4\lambda$) where a comparison is made between the infinite and finite width ($W = 1.4\lambda$) cases. In the first case only the geometrical optics term is needed while in the latter case equations (4.2.7) to (4.2.10) are employed. The comparison indicates that the pattern around $\theta = 0^\circ$ and up to $\theta = \pm 50^\circ$ can be reasonably predicted from the geometrical optics term. Beyond 50° the contribution of edge rays becomes significant. A similar comparison is given in Fig. 5.3 for the dielectric-loaded case ($\tau = 0.127\lambda$, $\varepsilon_r = 2.59$, $s = 0.4\lambda$) which indicates that edge rays in this case have more significant effect even at the axis of symmetry ($\theta = 0^\circ$). Thus, from (4.2.1) and (4.2.2) the geometrical optics normalized field at $\theta = 0^\circ$ is given by

$$E = e^{jk\bar{s}} + \Gamma_e(0)\, e^{-jk\bar{s}}$$

$$= e^{jk\bar{s}} + e^{-jk\bar{s}} + j\psi_e$$

where

$$\tan \psi_e = \frac{(1-r_e)\sin 2\delta'}{2r_e - (1+r_e)\cos 2\delta'}$$

E has a maximum value of 2 if $\psi_e = 2k\bar{s}$. As an example, if $\bar{s} = \frac{(2n+1)\lambda}{2}$, where $n = 0,1, \ldots,$ the dielectric slab should be chosen such that $\tau = \frac{0.25\lambda}{\sqrt{\varepsilon_r}}$. A set of calculations around

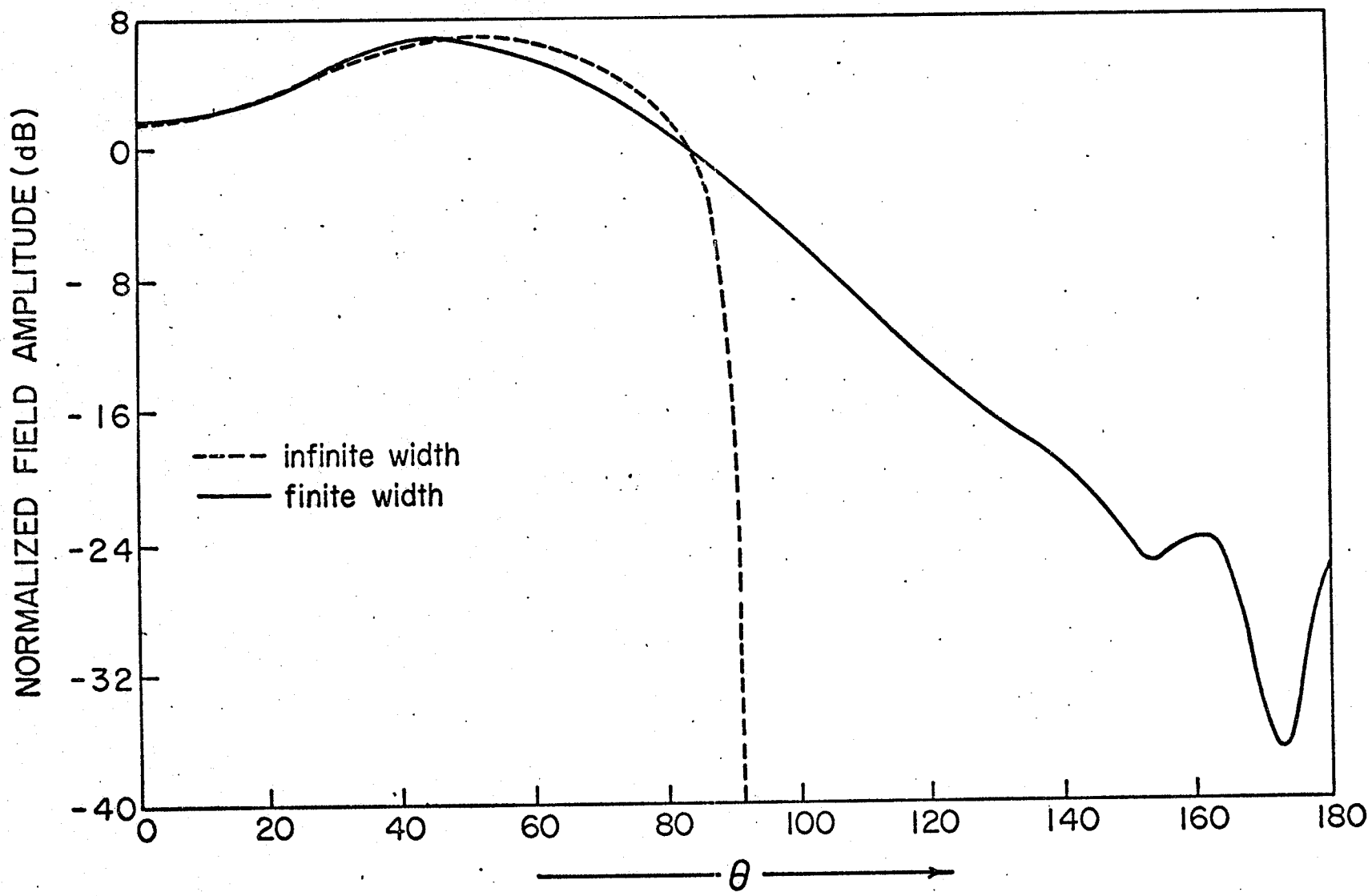

Fig. 5.2. Comparison between the radiation patterns of infinite and finite width (W = 1.4λ) unloaded strip (s = 0.4λ).

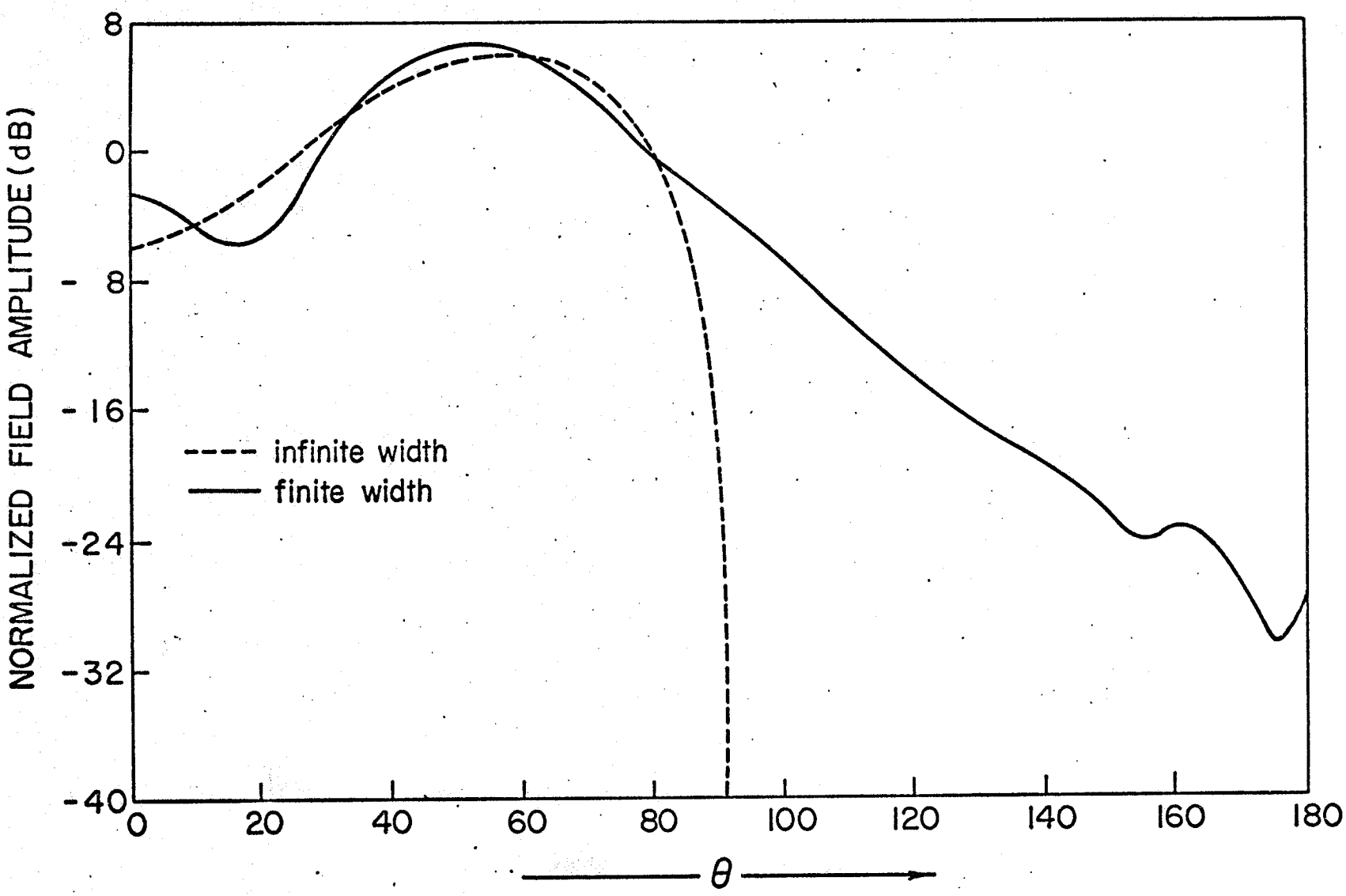

Fig. 5.3. Comparison between the radiation patterns of infinite and finite width (W = 1.4λ) loaded strip (s = 0.4λ, τ = 0.127λ, ε_r = 2.59).

this value of τ for $\varepsilon_r = 2.59$ and different strip widths (2W) was performed. The results indicate that there is an optimum value of τ for each W, e.g. this value is $\frac{0.21\lambda}{\sqrt{\varepsilon_r}}$ for $W = 0.9\lambda$ and equal to $\frac{0.25\lambda}{\sqrt{\varepsilon_r}}$ for $W = 1.6\lambda$, while for $W = 1.9\lambda$ the optimum value of τ is $\frac{0.28\lambda}{\sqrt{\varepsilon_r}}$. This conclusion indicates that the significance of edge ray contribution along the axis of symmetry is a function of W, and the inclusion of this contribution is necessary if high accuracy or optimum choice of τ are required.

Figure 5.4 shows a comparison between the loaded and unloaded strip and indicates that the pattern is changed due to the loading, more significantly within the range $\theta = \pm 50^\circ$. The forward field (at $\theta = 0^\circ$) is reduced by 3.5 dB and the back lobe radiation increases due to dielectric loading in this case. A similar comparison for $s = 0.62\lambda$ is presented in Fig. 5.5 and indicates an axial gain of 1.7 dB and a deterioration in the back lobe radiation for the loaded strip. The results of Figs. 5.4 and 5.5 indicate that the direction of scattered rays in each case is altered by the dielectric in a manner which suggests control of the pattern by means of the dimensions W, s, ε_r and τ.

The theoretical results for the strip are compared with a set of experimental data in section 4.3. The accuracy of the measurement is limited mainly by the contribution from those edges of the strip which are normal to the dipole axis, as well as reflections from the walls of the chamber. These

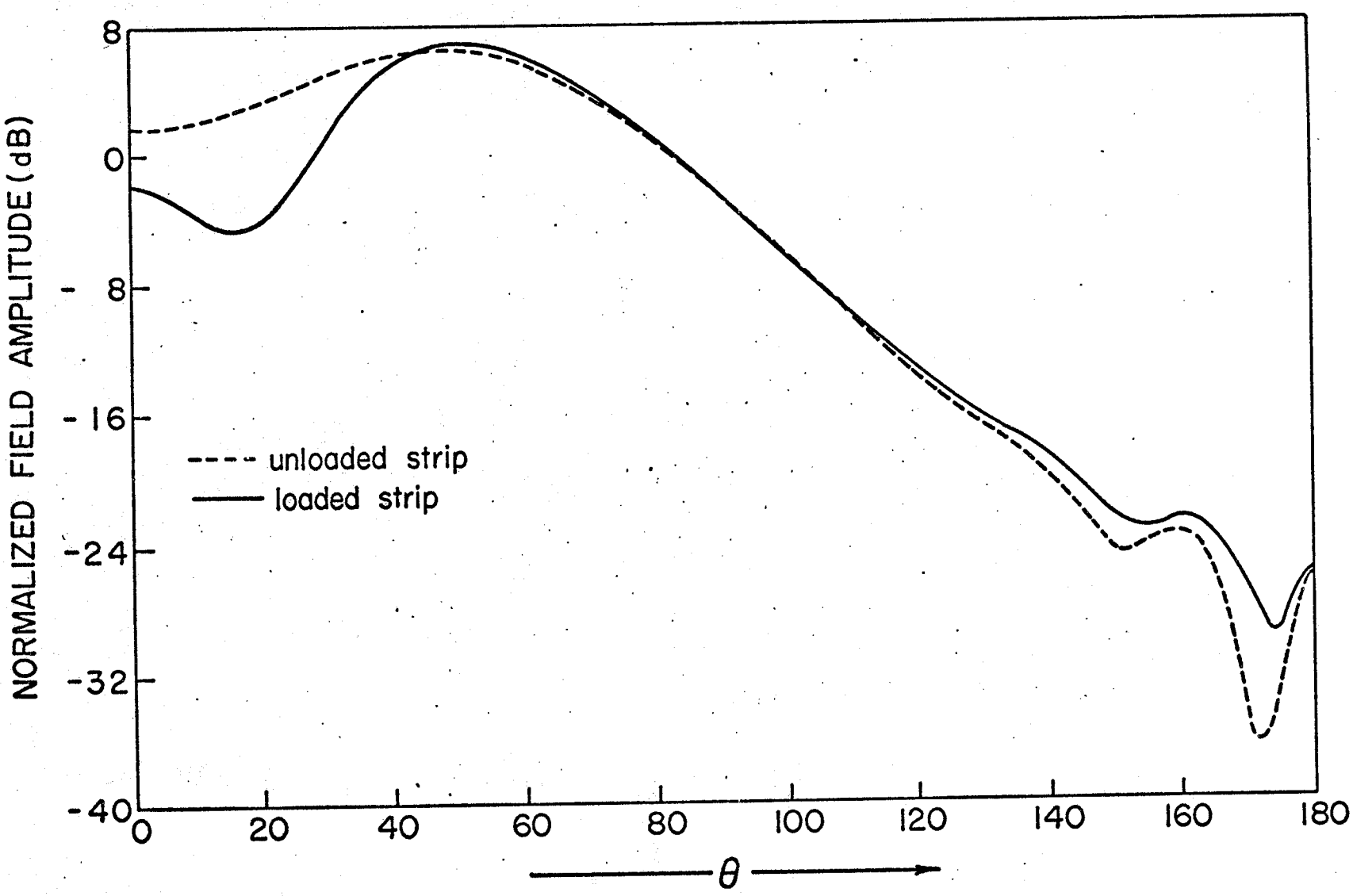

Fig. 5.4. Effect of dielectric loading on the radiation pattern of the strip ($s = 0.4\lambda$, $\tau = 0.127\lambda$, $\varepsilon_r = 2.59$).

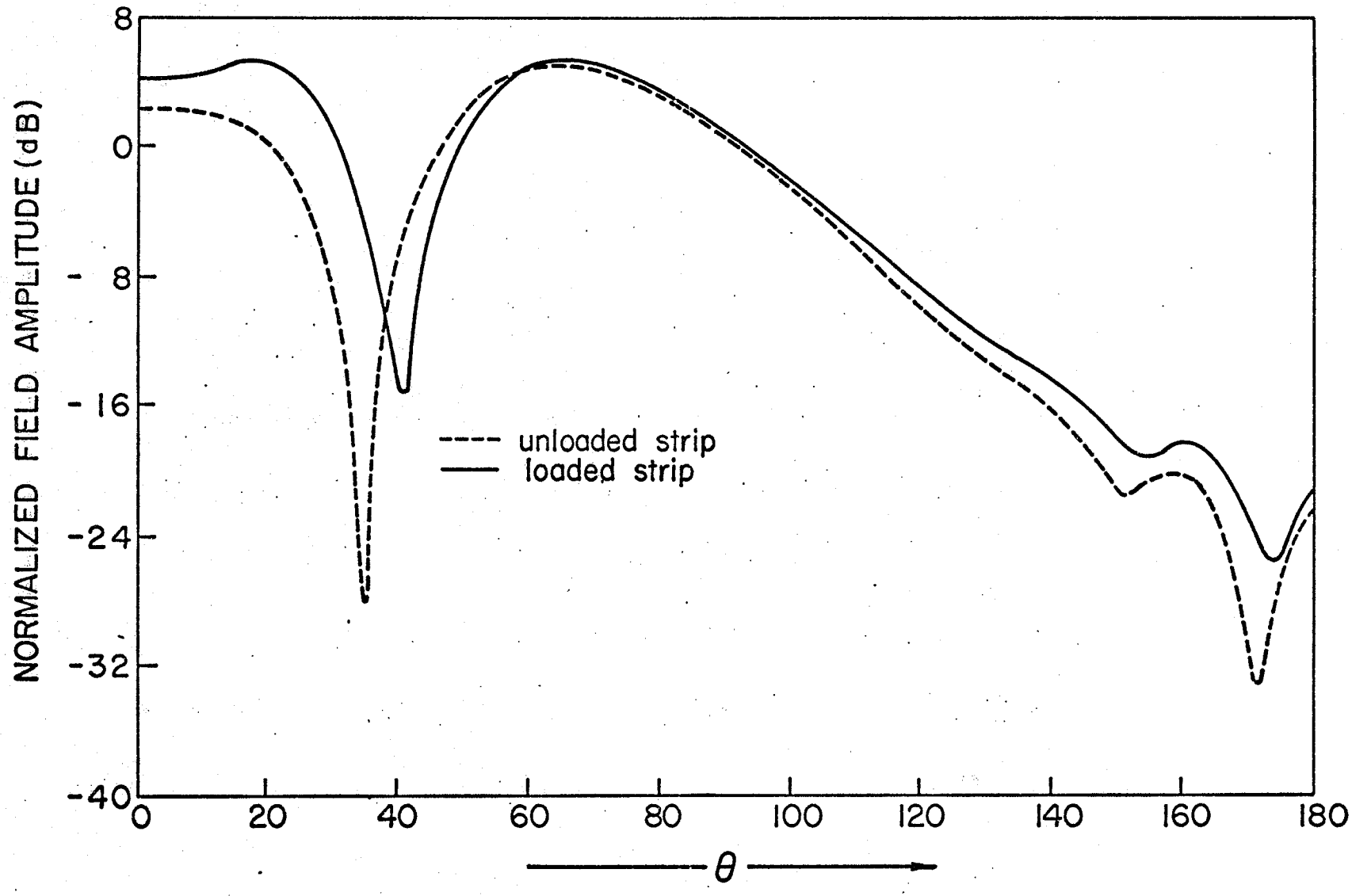

Fig. 5.5. Effect of dielectric loading on the radiation pattern of the strip ($s = 0.62\lambda$, $\tau = 0.127\lambda$, $\varepsilon_r = 2.59$).

two contributions are significant for low received signals, particularly for angles (θ) beyond 140°. Generally a good agreement between the theoretical and experimental data is found for all cases considered, as shown in Figs. 4.4 and 4.5, for both unloaded and loaded strips, respectively. It should be noted that the deviation in both cases is of the same order, which gives further confidence in our results for the loaded strip.

CHAPTER 6

CONCLUSIONS AND SUGGESTIONS FOR FUTURE RESEARCH

6.1 Conclusions

The main purpose of this thesis is to extend the applicability of the geometrical theory of diffraction to specific diffracting and scattering geometries. With this aim, the diffraction of waves by a perfectly conducting wedge with and without a thin dielectric loading, whose relative dielectric constant is not much larger than unity, is treated in integral form. Appropriate diffraction coefficients are obtained, using the saddle point technique, in terms of Fresnel's integral. Since the basic integrals are common to the loaded and unloaded wedges, and since the results for the unloaded wedge are in excellent agreement with the exact solution, it is concluded that the integration procedure is sufficiently accurate and may be employed with confidence in similar problems. Furthermore, the asymptotic diffraction theory, as developed here, is adequate for evaluating the field along shadow boundaries and for calculating near field edge-edge interactions.

Ray theory is employed to predict the radiation pattern of a dipole-fed strip loaded with a uniform dielectric slab. Good agreement between predicted and experimental

results is obtained over the range $\theta = 0°$ to $\theta = 140°$. Beyond $\theta = 140°$ experimental results become unreliable due to the increasing significance of reflections from the walls of the chamber and contributions from strip edges which are normal to the dipole axis. The results demonstrate that dielectric loading has significant effects on the radiation pattern even for the small thickness considered ($\tau = 0.127\lambda$, $\varepsilon_r = 2.59$). As an example, the field intensity along the axis of symmetry of the strip can increase by 1.7 dB (for $s = 0.62\lambda$) or decrease by 3.5 dB (for $s = 0.4\lambda$) due to dielectric loading. The importance of edge ray contributions, even along the axis of symmetry of the strip, is also demonstrated by considering the optimum thickness of the slab for given strip width, location of the source and relative permittivity. Thus, for $\bar{s} = \frac{\lambda}{2}$, $W = 0.9\lambda$, $\varepsilon_r = 2.59$ the optimum thickness is found to be $\tau = \frac{0.21\lambda}{\sqrt{\varepsilon_r}}$ instead of $\frac{0.25\lambda}{\sqrt{\varepsilon_r}}$ as obtained by considering only the geometrical optics contribution. For this optimum thickness an increase of the axial field of 4.1 dB is obtained. In general, the radiation pattern depends on the electrical and geometrical parameters of the dielectric loading.

6.2 Suggestions for Future Research

The solutions of the two canonical problems treated in this thesis have many other applications in structures with the same local characteristics as employed in the canonical problems, e.g. diffraction by double wedges, slits, strips, parallel-plate waveguides, corner reflectors and horn antennas. Such solutions can now take into account multiple reflections at the surfaces as well as edge-edge interactions with better accuracy.

The results for the dielectric-loaded strip indicate the dependence of the radiation pattern on the thickness as well as the dielectric constant of the loading. These parameters can be optimized in favor of certain radiation characteristics. The use of multiple dielectric slabs will widen the scope of the choice and may prove advantageous for certain applications.

Though our results for the dielectric-loaded strip are in good agreement with experiment, more accurate results may be expected if a more accurate solution for the problem of diffraction by a dielectric-loaded wedge is available. Such a solution may increase the range of applicability of the ray method to greater dielectric thicknesses and higher permittivities. A knowledge of the appropriate edge condition is essential for a rigorous approach to the solution. A method which appears somewhat promising for the case of dielectric-loaded half-plane is the Wiener-Hopf

technique which was applied by Jones [105] to solve for the case of a thick conducting half-plane.

APPENDIX A

INTEGRAL EXPRESSIONS FOR $I_\nu(a)K_\nu(b)$

The product $I_\nu(a)K_\nu(b)$ can have different integral representations. One such representation is given by [106, vol. 2, p. 53]

$$I_\nu(a)K_\nu(b) = \frac{1}{2}\int_0^\infty e^{-(x + \frac{a^2+b^2}{4x})} I_\nu(\frac{ab}{2x}) \frac{dx}{x} \qquad (A.1)$$

Using the integral form of $I_\nu(z)$ [107, p. 181], i.e.

$$I_\nu(z) = \frac{1}{2\pi j}\int_{\infty-j\pi}^{\infty+j\pi} e^{z\cosh w - \nu w} dw, \quad |\arg z| < \frac{\pi}{2} \qquad (A.2)$$

where the contour of integration joins the points $(\infty-j\pi)$, $(-j\pi)$, $(+j\pi)$ and $(\infty+j\pi)$ by straight lines, we obtain

$$I_\nu(a)K_\nu(b) = \frac{1}{4\pi j}\int_0^\infty \frac{e^{-(x + \frac{a^2+b^2}{4x})}}{x} \int_{\infty-j\pi}^{\infty+j\pi} e^{\frac{ab}{2x}\cosh w - \nu w} dw\, dx \qquad (A.3)$$

Interchanging the order of integrations and utilizing the integral form of MacDonald's function [106, p. 82], i.e.

$$K_\nu(z) = \frac{1}{2}\int_0^\infty \frac{e^{-(x + \frac{z^2}{4x})}}{x^{\nu+1}} dx$$

it may be shown that (A.3) reduces to

$$I_\nu(a)K_\nu(b) = \frac{1}{2\pi j}\int_{\infty-j\pi}^{\infty+j\pi} e^{-\nu w}\, K_0\{(a^2+b^2-2ab\cosh w)^{\frac{1}{2}}\}\, dw \qquad (A.4)$$

Substituting $w = \zeta - j\pi$ along the line C_1 joining $(\infty-j\pi)$ and $(-j\pi)$, and letting $w = \zeta + j\pi$ along C_2 which joins $(j\pi)$ and $(\infty+j\pi)$ we obtain

$$\{\int_{C_1} + \int_{C_2}\}\{e^{-\nu w}\, K_0[(a^2+b^2-2ab\cosh w)^{\frac{1}{2}}]\}\, dw$$

$$= \frac{1}{2\pi j}\int_0^\infty \{e^{-\nu(\zeta+j\pi)} - e^{-\nu(\zeta-j\pi)}\}K_0[(a^2+b^2+2ab\cosh \zeta)^{\frac{1}{2}}]\, d\zeta$$

$$= -\frac{\sin \nu\pi}{\pi}\int_0^\infty e^{-\nu\zeta}\, K_0[(a^2+b^2+2ab\cosh \zeta)^{\frac{1}{2}}]\, d\zeta$$

Letting $w = -j\zeta$ along C_3 joining the points $(-j\infty)$, and (0) and letting $w = j\zeta$ along C_4 which joins the points (0) and $(j\infty)$, we obtain

$$\{\int_{C_3} + \int_{C_4}\}\{e^{-\nu w}\, K_0[(a^2+b^2-2ab\cosh w)^{\frac{1}{2}}]\}\, dw$$

$$= \frac{1}{2\pi}\int_0^\pi \{e^{-j\nu\zeta} + e^{j\nu\zeta}\}\, K_0[(a^2+b^2-2ab\cos \zeta)^{\frac{1}{2}}]\, d\zeta$$

$$= \frac{1}{\pi}\int_0^\pi \cos \nu\zeta\, K_0[(a^2+b^2-2ab\cos \zeta)^{\frac{1}{2}}]\, d\zeta \qquad (A.5)$$

Now, the product in (A.1) takes the form

$$\pi I_\nu(a)K_\nu(b) = \int_0^\pi \cos \nu\zeta \; K_0\{(a^2+b^2-2ab\cos \zeta)^{\frac{1}{2}}\} \, d\zeta$$
$$- \sin \nu\pi \int_0^\infty e^{-\nu\zeta} \; K_0\{(a^2+b^2+2ab\cosh \zeta)^{\frac{1}{2}}\} \, d\zeta \qquad \text{(A.6)}$$

This equation was derived by Oberhettinger [67] using a different procedure.

APPENDIX B

DERIVATION OF EQUATION (3.2.14)

In order to derive (3.2.14) we let

$$\bar{I} = \int_0^\infty K_{j\mu}(\gamma r)\, \frac{\sinh \mu\beta}{\sinh \mu\alpha}\, d\mu \tag{B.1}$$

Replacing $K_{j\mu}(\gamma r)$ by the integral [89, p. 376]

$$K_{j\mu}(\gamma r) = \int_0^\infty e^{-\gamma r \cosh x} \cos \mu x\, dx$$

and interchanging the order of integration we get

$$\bar{I} = \int_0^\infty e^{-\gamma r \cosh x} \int_0^\infty \frac{\sinh \mu\beta}{\sinh \mu\alpha} \cos \mu x\, d\mu\, dx \tag{B.2}$$

The integration over μ can be evaluated [91, p. 504] to be

$$\int_0^\infty \frac{\sinh \mu\beta}{\sinh \mu\alpha} \cos \mu x\, d\mu = \frac{\pi}{2\alpha} \frac{\sin\frac{\pi\beta}{\alpha}}{\cosh\frac{\pi x}{\alpha} + \cos\frac{\pi\beta}{\alpha}}\,, \quad -\alpha<\beta<\alpha$$

and hence $\bar{I}$ may be written in the form

$$\bar{I} = \frac{\pi}{2\alpha} \sin\frac{\pi\beta}{\alpha} \int_0^\infty \frac{e^{-\gamma r \cosh x}}{\cosh\frac{\pi x}{\alpha} + \cos\frac{\pi\beta}{\alpha}}\, dx, \quad -\alpha<\beta<\alpha \tag{B.3}$$

REFERENCES

1. Keller, J.B., "The geometric optics theory of diffraction," Proc. of the 1953 McGill Symposium on Microwave Optics, edited by B.S. Karsik. Bedford: Air Force Cambridge Research Center, Part II, pp. 207-210, April 1959.

2. Keller, J.B., "A geometrical theory of diffraction," in Calculus of Variations and Its Applications, Proc. of the Symp. in Applied Mathematics, vol. 8, edited by L.M. Graves, New York: McGraw-Hill Co. Inc., pp. 27-52, 1958.

3. Keller, J.B., "Geometrical theory of diffraction," J. Opt. Soc. Am., vol. 52, No. 2, pp. 116-130, February 1962.

4. Jones, D.S., The Theory of Electromagnetism. London: Pergamon Press, 1964.

5. Felsen, L.B., "Quasi-optics diffraction," in Proc. of the Symp. on Quasi-optics, Microwave Research Inst. Symp. Series, vol. 14, edited by J. Fox. New York: Polytechnic Press, pp. 1-41, 1964.

6. Levy, B.R. and Keller, J.B., "Diffraction by a smooth object," Com. Pure and Appl. Math., vol. 12, pp. 159-209, January 1959.

7. Keller, J.B., "Diffraction by an aperture," J. Appl. Phys., vol. 28, pp. 426-444, April 1957.

8. Kapany, N.S., Burke, J.J. and Frame, K., "Diffraction by apertures of wavelength dimensions," Appl. Optics, vol. 4, pp. 1229-1238, October 1965.

9. Mohsen, A. and Hamid, M.A.K., "On higher order asymptotic terms of the two-dimensional diffraction by a small aperture," Radio Science, vol. 3, pp. 1105-1108, November 1968.

10. Balanis, C.A., "Radiation from slots on cylindrical bodies using geometrical theory of diffraction and creeping wave theory," Ph.D. thesis, Dept. Elect. Eng'g., The Ohio State University, Columbus, Ohio, 1969.

11. Lysher, L.J., "A study of the near field behind a parabolic antenna," M.Sc. thesis, The Ohio State University, Columbus, Ohio, 1961.

12. Kinber, B. Ye, "The role of diffraction at the edges of a paraboloid in fringe radiation," Radio Eng'g. and Electronic Phys., vol. 7, pp. 79-86, January 1962.

13. Kinber, B. Ye, "Diffraction at the open end of a sectoral horn," Radio Eng'g. and Electronic Phys., vol. 7, pp. 1620-1632, November 1962.

14. Kinber, B. Ye, "Contribution to the theory of flat horns having rounded edges," Radio Eng'g. and Electronic Phys., vol. 8, pp. 1923-1927, December 1963.

15. Russo, P.M., Rudduck, R.C., and Peters, L. Jr., "A method for computing E-plane pattern of horn antennas," IEEE Trans. Antennas Propagat., vol. AP-13, pp. 219-224, March 1965.

16. Hamid, M.A.K., "Near field transmission between horn antennas," Elect. Eng'g. Dept., University of Toronto, Toronto, Research Rept. No. 43, 1966.

17. Hamid, M.A.K., "Diffraction by a conical horn," IEEE Trans. Antennas Propagat., vol. AP-16, pp. 520-528, September 1968.

18. Jull, E.V., "A revision of Shelkunoff's expression for the gain of pyramidal horn," 1969 IEEE/G-AP International Symp., Austin, Texas, pp. 286-289.

19. Hutchins, D.L. and Kouyoumjian, R.G., "Calculation of the field of a baffled array by the geometrical theory of diffraction," J. Accous. Soc. Am., vol. 45, No. 2, pp. 485-492, February 1969.

20. Ryan, C.E., Jr. and Rudduck, R.C., "A wedge diffraction analysis of the radiation patterns of parallel-plate waveguides," IEEE Trans. Antennas Propagat., vol. AP-16, pp. 490-491, July 1968.

21. Rudduck, R.C., "Application of wedge diffraction to antenna theory," Antenna Lab., The Ohio State University, Columbus, Ohio, Rept. No. 1691-13, 1965.

22. Rudduck, R.C. and Tsai, L.L., "Aperture reflection coefficient of TEM and TE_{10} Mode Parallel-plate Waveguides," IEEE Trans. Antennas Propagat., vol. AP-16, pp. 83-89, January 1968.

23. Hamid, M.A.K., "Reflection coefficient at a horn waveguide junction," IEEE Trans. Antennas Propagat., vol. AP-15, pp. 264-265, July 1967.

24. Jones, J.E., Tsai, L.L., Rudduck, R.C., Swift, C.T., and Burnside, W.D., "The admittance of a parallel-plate waveguide aperture illuminating a metal sheet," IEEE Trans. Antennas Propagat., vol. AP-16, pp. 528-535, September 1968.

25. Yee, H.Y., "Ray-optical techniques for waveguide discontinuities," Ph.D. thesis, Microwave Research Inst., Polytech. Inst. of Brooklyn, New York, N.Y., 1968.

26. Yee, H.Y., Felsen, L.B., and Keller, J.B., "Ray theory of reflection from the open end of a waveguide," SIAM J. Appl. Math., vol. 16, pp. 268-300, March 1968.

27. Yee, H.Y. and Felsen, L.B.,"Ray-optics - a novel approach to scattering by discontinuities in a waveguide," IEEE Trans. Microwave Theory and Technique, vol. MTT-17, pp. 73-85, January 1969.

28. Yee, H.Y. and Felsen, L.B., "Ray-optical analysis of electromagnetic scattering in waveguides," IEEE Trans. Microwave Theory and Technique, vol. MTT-17, pp. 671-683, September 1969.

29. Lewin L. and Grain, G.E., "Theoretical performance of the overmoded right-angle corner," Proc. IEE, vol. 116, pp. 667-678, May 1969.

30. Balanis, C.A., "Pattern distortion due to edge diffractions," IEEE Trans. Antennas Propagat., vol. AP-18, pp. 561-563, April 1970.

31. Mohsen, A. and Hamid, M.A.K., "Ray-optical diffraction coefficients for waveguide discontinuity problems," presented at the International Microwave Symposium, Los Angeles, California, 1970.

32. Ufimtsev, P. Ia, "Approximate computation of the diffraction of plane electromagnetic wave at certain metal bodies. I - Diffraction patterns at a wedge and a ribbon," Soviet Phys. Tech. Phys., vol. 2, pp. 1708-1718, August 1957.

33. Ufimtsev, P. Ia, "Secondary diffraction of electromagnetic waves by a strip," Soviet Phys. Tech. Phys., vol. 3, pp. 535-548, March 1958.

34. Yu, J.S. and Rudduck, R.C., "On higher order diffraction concepts applied to a conducting strip," IEEE Trans. Antennas Propagat., vol. AP-15, pp. 662-668, September 1967.

35. Mohsen, A. and Hamid, M.A.K., "Modified asymptotic solution for the two-dimensional scattering by a conducting strip," Electronic Letters, vol. 6, pp. 12-13, January 1970.

36. Ufimtsev, P. Ia, "Secondary diffraction of electromagnetic waves by a disk," Soviet Phys. Tech. Phys., vol. 3, pp. 549-556, March 1958.

37. Bechtel, M.E., "Application of geometrical diffraction theory to scattering from cones and disks," Proc. IEEE, vol. 53, pp. 877-882, August 1965.

38. Burke, J.E. and Keller, J.B., "Diffraction by a thick screen, a step and related axially symmetrical objects," Electronic Defence Lab., Mountain View, California, Eng'g. Rept. No. EDL-E98, 1960.

39. Morse, B.J., "Diffraction by polygonal cylinders," J. Mathematical Phys., vol. 15, No. 2, pp. 199-214, February 1964.

40. Balanis, C.A., "Radiation characteristics of current elements near a finite length cylinder," IEEE Trans. Antennas Propagat., vol. AP-18, pp. 352-359, May 1970.

41. Ross, R.A., "Bistatic scattering matrix for a frustum," IEEE Trans. Antennas Propagat., vol. AP-17, pp. 103-106, January 1969.

42. Ross, R.A., "Small angle scattering by a cone," IEEE Trans. Antennas Propagat., vol. AP-17, pp. 241-242, March 1969.

43. Pauli, W., "On asymptotic series for function in the theory of diffraction of light," Phys. Rev., vol. 54, pp. 924-931, December 1938.

44. Buchal, R.N. and Keller, J.B., "Boundary layer problems in diffraction theory," Com. Pure and Appl. Math., vol. 13, No. 1, pp. 84-114, February 1960.

45. Ahluwalia, D.S., Lewis, R.M., and Boersma, J., "Uniform asymptotic theory of diffraction by a plane screen," SIAM J. Appl. Math., vol. 16, pp. 783-807, July 1968.

46. Lewin, L., "Wedge diffraction functions and their use in quasioptics, "Proc. IEE, vol. 116, pp. 71-76, January 1969.

47. Sommerfeld, A., "Mathematische Theorie der Diffraktion," Math. Annalen, vol. 47, pp. 317-341, 1896.

48. Sommerfeld, A., "Über Verzureigte Potentiale im Raum," Proc. London Math. Soc (1), vol. 28, pp. 395-429, 1897.

49. Sommerfeld, A., "Theoretisches über der Beugung der Roentgenstrahlen," Z. fur Math und Physik, vol. 46, pp. 11-97, 1901.

50. Sommerfeld, A., "Asymptotische Darstellung von Formeln aus der Beugungtheorie des Lichts," J. Reine Angew. Math., vol. 158, pp. 199-208, 1928.

51. Carslaw, H.S., "Some multiform solutions of the partial differential equations of physics and mathematics and their applications," Proc. London Math. Soc. (1), vol. 30, pp. 121-163, 1899.

52. Carslaw, H.S., "Oblique incidence of a train of plane waves on a semi-infinite plane," Proc. Edin. Math. Soc., vol. 19, pp. 71-77, June 1901.

53. Macdonald, H.M., "Electric waves," Appendix D. London: Cambridge University Press, 1902.

54. Carslaw, H.S., "Use of contour integration in the problem of diffraction by a wedge of any angle," Phil. Mag., vol. 5, pp. 374-379, March 1903.

55. Wiegrefe, A., "Über einige mehrwertige Lösungen der Wellengleichung $\Delta u + k^2 u = 0$ und ihre Anwendung in der Beugungstheorie," Ann. Physik, vol. 39, pp. 449-484, September 1912.

56. Macdonald, H.M., "A class of diffraction problems," Proc. London Math. Soc. (2), vol. 14, pp. 410-427, January 1915.

57. Carslaw, H.S., "Diffraction of waves by a wedge of any angle," Proc. London Math. Soc. (2), vol. 18, pp. 291-306, February 1920.

58. Bromwich, T.J.I'A., "Diffraction of waves by a wedge," Proc. London Math. Soc. (2), vol. 14, pp. 450-463, May 1915.

59. Hanson, E.T., "The shadow of a straight edge," Phil. Trans. Roy. Soc., vol. A237, pp. 35-65, February 1938.

60. Nomura, Y., "On the diffraction of electric waves by a perfectly reflecting wedge," Res. Inst., Tohoku Univ., Japan, Sci. Rept. Ser. B, vol. 1, pp. 1-23, January 1951.

61. Nomura, Y., "On the complete theory of diffraction of electromagnetic waves by a perfectly conducting wedge," Res. Inst., Tohoku Univ., Japan, Sci. Rept. Ser. B, vol. 1, pp. 29-50, January 1951.

62. Herglotz, G., "Die Greensche Funktion der Wellengleichung fur eine Keilformige Begrenzung," Math. Ann., vol. 124, pp. 219-234, 1952.

63. Tuzhilin, A.A., "New representation of diffraction fields in wedge-shaped regions with ideal boundaries," Sov. Phys. - Acoustics, vol. 9, No. 2, pp. 168-172, October-December 1963.

64. Kontorovich, M.J. and Lebedev, N.N., "On a method of solution of some problems in the diffraction theory," J. of Phys., Moscow, vol. 1, pp. 229-241, 1939.

65. Garnir, H.G., "Fonction de Green de l'opérateur métaharmonique pour les problèms de Dirichlet et de Neumann posés dans un angle au un dièdre," Bull. Soc. Roy. Sci., Liege (Belgium), vol. 21, pp. 119-140 and 207-231, 1952.

66. Oberhettinger, F., "Diffraction of waves by a wedge," Com. Pure and Appl. Math., vol. 7, pp. 551-563, August 1954.

67. Oberhettinger, F., "On the diffraction and reflection of waves and pulses by wedges and corners," J. of Research, Nat. Bureau of Standards (U.S.A.), vol. 61B, pp. 343-365, November 1958.

68. Felsen, L.B., "Alternative field representation in regions bounded by spheres, cones and planes," IEEE Trans. Antennas Propagat., vol. AP-5, No. 1, pp. 109-121, January 1957.

69. Williams, W.E., "A class of boundary value problems," Appl. Sci. Res. (B), vol. 9, pp. 21-34, 1961.

70. Faulker, T.R., "Diffraction of singular fields by a wedge," Arch. Rat. Mech. Analysis, vol. 18, pp. 196-204, 1965.

71. Wait, J.R. and Jackson, C.M., "Calculations of the field near the apex of a wedge surface," Nat. Bureau of Standards, Tech. Note No. 204, November 1963.

72. Harrington, R.F.,Time-harmonic Electromagnetic Fields. New York: McGraw-Hill Co. Inc., 1961.

73. Jackson, W.H., "On the diffraction of light produced by an opaque prism of finite angle," Proc. London Math. Soc. (2), vol. 1, pp. 393-414, January 1904.

74. Reiche, F., "Diffraction of light at a plane rectangular corner of infinite conductivity," Ann. der Phys., vol. 37, pp. 131-156, December 1911.

75. Ott, H., "Die Sattelpunktsmethode in der Umgebung eines Poles mit Anwending aus die Wellenoptik und Akustik," Annalen der Phys., vol. 43, pp. 393-403, 1943.

76. Clemmow, P.C., "Some extensions to the method of integration by steepest descents," Quart. J. Mech. and Appl. Math., vol. 3, pp. 241-256, 1950.

77. Oberhettinger, F., "On asymptotic series for functions occurring in the theory of diffraction of waves by wedges," J. Math. Phys., vol. 34, pp. 245-255, 1955-1956.

78. Oberhettinger, F., "On a modification of Watson's lemma," J. of Research of the Nat. Bureau of Standards, vol. 63B, pp. 15-17, 1959.

79. Van der Waerden, B.L., "On the method of saddle points," Appl. Sci. Res. (B), vol. B2, pp. 33-45, 1951.

80. Hutchins, D.L. and Kouyoumjian, R.G., "Asymptotic series describing the diffraction of a plane wave by a wedge," Electroscience Lab., The Ohio State University, Columbus, Ohio, Sci. Rept. No. 3, December 1969.

81. Wait, J.R., "On the theory of an antenna with infinite corner," Can. J. Phys., vol. 32, pp. 365-371, June 1954.

82. Dybdal, R.B., "Mutual coupling between TEM and TE_{01} parallel plate waveguide aperture," Antenna Lab., The Ohio State University, Rept. 1693-5, August 1964.

83. Tsai, L.L. and Rudduck, R.C., "Accuracy of approximate formulations for near field wedge diffraction of a line source," Antenna Lab., The Ohio State University, Columbus, Ohio, Rept. 1691-18, March 1966.

84. Felsen, L.B. and Marcuwitz, N., "Modal analysis and synthesis of electromagnetic fields," Microwave Res. Inst., Polytech, Inst. Brooklyn, New York, N.Y., Rept. PIB MRI-1083-62, 1962.

85. Ufimtsev, P. Ia, "Transverse diffusion for diffraction by a wedge," Radio Eng'g and Electronic Phys., vol. 10, No. 6, pp. 866-875, June 1965.

86. Hutchins, D.L., "Asymptotic series describing the diffraction of a plane wave by a two-dimensional wedge of arbitrary angle," Ph.D. thesis, Dept. Elect. Eng'g., The Ohio State University, Columbus, Ohio, 1967.

87. Meixner, J. "Die Kantenbedingung in der Theorie der Beugung Electromagnetischer Wellen an vollkommen leitenden ebenen Schirmen," Ann. der Phys., vol. 6, No. 6, pp. 2-9, 1949.

88. Meixner, J., "The behaviour of electromagnetic fields at edges," Mathematical Sciences Institute, New York University, New York, N.Y., Rept. No. EM-72, 1954.

89. Abramowitz, M. and Stegun, I.A., Handbook of Mathematical Function with Formulas, Graphs and Mathematical Tables. Washington: U.S. Gov't. Print. Office, 1964.

90. Korn, G.A. and Korn, T.K., Mathematical Handbook for Scientists and Engineers. New York: McGraw-Hill Co. Inc., 1961.

91. Gradshtein, I.S. and Ryzhik, L.M., Tables of Integrals, Series and Products. New York: Academic Press, 1965.

92. Clemmow, P.C., "A note on the diffraction of a cylindrical wave by a perfectly conducting half plane," Quart. J. Mech. and Appl. Math., vol. 3, pp. 377-384, 1950.

93. Mohsen, A., "A note on Oberhettinger's solution for the scalar diffraction by a wedge," IEEE Trans. Education, vol. E-13, p. 122, August 1970.

94. Born, M. and Wolf, E., Principles of Optics. New York: The MacMillan Company, 1964.

95. Whipple, F.J.W., "Diffraction by a wedge and kindred problems," Proc. London Math. Soc.(2), vol. 16, pp. 94-111, December 1916.

96. Ohba, Y., "On the radiation pattern of a corner reflector finite in width," IEEE Trans. Antennas Propagat., vol. AP-11, pp. 127-132, March 1963.

97. Silver, S., Microwave Antenna Theory and Design. New York: McGraw-Hill Co. Inc., Ch. 11, 1949.

98. Hamid, M.A.K. and Mohsen, A., "Diffraction by dielectric-loaded horns and corner reflectors," IEEE Trans. Antennas Propagat., vol. AP-17, pp. 660-662, September 1969.

99. Tai, C.T., "The effect of a ground slab on the radiation from a line source," J. Appl. Phys., vol. 22, pp. 405-414, April 1951.

100. Pistol'kors, A.A., Kaplun, V.A. and Knyazeva, L.V., "On the diffraction of electromagnetic waves at dielectric or semi-conducting sheets," Radio Eng'g. and Electronic Phys., vol. 4, No. 6, pp. 1-13, June 1959.

101. Khrebet, N.G., "Diffraction of plane electromagnetic waves on the edge of a dielectric half-plane," Radio Eng'g. and Electronic Phys., vol. 13, No. 3, pp. 331-338, March 1968.

102. Lebedev, N.N., "Sur une fomule d'inversion," Comptes Rendus (Dokaldy) de l'Academie de Sciences de l'URSS, vol. 52, pp. 655-658, 1946.

103. Morse, P.M. and Feshback, H., Methods of Mathematical Function. New York: McGraw-Hill Co. Inc., 1953.

104. Ohba, Y., "Directional characteristics of a dipole antenna with a rectangular reflector," J. Appl. Phys. (Japan), vol. 26, pp. 11-17, January 1957.

105. Jones, D.S., "Diffraction by a thick semi-infinite plate," Proc. Roy. Soc. (London), vol. 217A, pp. 153-175, April 1953.

106. Erdelyi, A., Magnus, W., Oberhettinger, F. and Tricomi, F.G., Higher Transcendental Functions. New York: McGraw-Hill Co. Inc., 1953.

107. Watson, G.N., A Treatise on the Theory of Bessel Functions. London: Cambridge University Press, second edition, 1944.